Analysis and simulations of coupled bulk-surface reaction-diffusion systems on exponentially evolving volumes

Article (Accepted Version)

Analysis and simulations of coupled bulk-surface reaction-diffusion systems on exponentially evolving volumes

A. Madzvamuse,*[1] and A. H. Chung[2]

[1] University of Sussex, School of Mathematical and Physical Sciences, Department of Mathematics, Pevensey III, 5C15, Brighton, BN1 9QH, UK

[2] 34-36 St. Georges Road, Brighton, BN2 1ED, UK

Abstract. In this article we present a system of coupled bulk-surface reaction-diffusion equations on exponentially evolving volumes. Detailed linear stability analysis of the homogeneous steady state is carried out. It turns out that due to the nature of the coupling (linear Robin-type boundary conditions) the characterisation of the dispersion relation in the absence and presence of spatial variation (i.e. diffusion), can be decomposed as a product of the dispersion relation of the bulk and surface models thereby allowing detailed analytical tractability. As a result we state and prove the conditions for diffusion-driven instability for systems of coupled bulk-surface reaction-diffusion equations. Furthermore, we plot explicit evolving parameter spaces for the case of an exponential growth. By selecting parameter values from the parameter spaces, we exhibit pattern formation in the bulk and on the surface in complete agreement with theoretical predictions.

Keywords and phrases: Coupled bulk-surface reaction-diffusion systems, Bulk-surface finite element method, Diffusion-driven instability, Evolving domains/volumes and surfaces, Fractional-step θ method

Mathematics Subject Classification: 35Q53, 34B20, 35G31

1. Introduction to coupled bulk-surface partial differential equations

The coupling of bulk and surface dynamics through the use of partial differential equations (PDEs) in multi-dimensions is prevalent in many cellular biological systems and fluid dynamics [3, 5, 8, 15, 28, 29, 32, 33, 35, 36] as well as in other exotic areas of solid mechanics such as topological insulator thin films [9] and in large- and small-scale atmospheric and coupled ocean-atmosphere models for air-sea interactions [4]. In the areas of cellular and developmental biology, in many of these applications and processes, the formation of heterogeneous distributions of chemical substances emerge through symmetry breaking of morphological instabilities [17]. For example, it is essential the emergence and maintenance of polarised states in the form of heterogeneous distributions of chemical species such as proteins and lipids. Examples of such processes include (but are not limited to) the formation of buds in yeast cells and cell polarisation

*Corresponding author. E-mail: a.madzvamuse@sussex.ac.uk

in biological cells due to responses to external signals through the outer cell membrane [35, 36]. In the context of reaction-diffusion processes, such symmetry breaking arises when a uniform steady state, stable in the absence of diffusion, is driven unstable when diffusion is present thereby giving rise to the formation of spatially inhomogeneous solutions in a process now well-known as the Turing diffusion-driven instability [41]. Classical Turing theory requires that one of the chemical species, typically the *inhibitor*, diffuses much faster than the other, the *activator*, resulting in what is known as the *long-range inhibition* and *short-range activation* [10, 30].

Recently, there has been a surge in studies on models that couple bulk and surface dynamics. For example, Hahn et al. [11] model the surfactant concentration by use of a coupled bulk-surface model, and Rätz and Röger [36] study symmetry breaking in a bulk-surface reaction-diffusion model for signalling networks. In the former work, a reaction-convenction-diffusion is proposed that couples the concentrations of surfactants in the bulk (a single PDE) and on the free surfaces (a single PDE), while in the latter work, a single diffusion partial differential equation (the heat equation) is formulated inside the bulk of a cell, while on the cell-surface, a system of two membrane reaction-diffusion equations is formulated. The bulk and cell-surface membrane are coupled through Robin-type boundary conditions and a flux term for the membrane system [36]. Elliott and Ranner [7] study a finite element approach to a sample elliptic problem: a single elliptic partial differential equation is posed in the bulk and another is posed on the surface. These are then coupled through Robin-type boundary conditions. Novak et al. [33] present an algorithm for solving a diffusion equation on a curved surface coupled to a diffusion model in the volume. Checkkin et al. [5] study bulk-mediated diffusion on planar surfaces. Again, diffusion models are posed in the bulk and on the surface coupling them through boundary conditions. In the area of tissue engineering and regenerative medicine, electrospun membrane are useful in applications such as filtration systems and sensors for chemical detection. Understanding of the fibres' surface, bulk and architectural properties is crucial to the successful development of integrative technology. Nisbet et al. [32] present a detailed review on surface and bulk characterisation of electrospun membranes of porous and fibrous polymer materials. To explain the long-range proton translocation along biological mombranes, Medvedev and Stuchebrukhov [29] propose a model that takes into account the coupled bulk-diffusion that accompanies the migration of protons on the surface. More recently, Rozada *et al.,* [37] present singular perturbation theory for the stability of localised spot patterns for the Brusselator model on the sphere.

In most of the work above, either elliptic or diffusion models in the bulk have been coupled to surface-elliptic or surface-diffusion or surface-reaction-diffusion models posed on the surface through Robin-type boundary conditions [5, 8, 29, 32, 33, 35, 36]. Recently, we proposed and developed a new mathematical framework for coupled bulk-surface reaction-diffusion systems [24, 26] on stationary domains and volumes. In a similar study, Macdonald et al. [19] proposed a computational framework to study coupled bulk-surface reaction-diffusion models on evolving domains and manifolds with applications to cell migration and chemotaxis. Nagata et al. [31] studied reaction-diffusion systems with applications to plant tip morphogenesis bifurcations on spherical caps.

In this work, we introduce domain growth and derive the conditions for Turing domain-growth diffusion-driven instability for the special case of uniform isotropic exponential growth. Our motivation is to couple systems of reaction-diffusion equations posed in the bulk and on the surface which are continuously evolving in space and time, setting a mathematical and computational framework to study more complex interactions such as those observed in cell biology, tissue engineering, regenerative medicine, developmental biology and biopharmaceuticals [5, 8, 29, 32, 33, 35, 36, 44].

To numerically solve the coupled model system, we employ the evolving bulk-surface finite element method which is an extension of the bulk-surface finite element method introduced earlier for solving a coupled system of reaction-diffusion equations on stationary domains and volumes [26]. The bulk-surface finite element method was first introduced by Elliott and Ranner in [7] to numerically solve the coupled system of bulk-surface reaction-diffusion equations. Details of the surface-finite element can be found in [6]. The bulk and surface reaction-diffusion systems are coupled through Robin-type boundary conditions. The coupled bulk-surface finite element algorithm is implemented in **deall II** [1].

Our mathematical and computational framework generalises substantially the theory of pattern formation in the following ways:

- We derive and prove Turing diffusion-driven instability conditions for a coupled system of bulk-surface reaction-diffusion equations on exponentially evolving volumes.
- We compute explicit domain growth induced parameter spaces in order to identify appropriate model parameters.
- Using a bulk-surface finite element method, we approximate the solution to the model system within the bulk and on the boundary surface of an evolving sphere of radius one.
- Our results show that if the surface-reaction-diffusion system has the *long-range inhibition, short-range activation* form (i.e. $d_\Gamma > 1$) and the bulk-reaction-diffusion system has equal diffusion coefficients (i.e. $d_\Omega = 1$), then the surface-reaction-diffusion system can induce patterns in the bulk close to the surface and no patterns form in the interior, far away from the surface.
- On the other hand, if the bulk-reaction-diffusion system has the *long-range inhibition, short-range activation* form (i.e. $d_\Omega > 1$) and the surface-reaction-diffusion system has equal diffusion coefficients (i.e. $d_\Gamma = 1$), then the bulk-reaction-diffusion system can induce pattern formation on the surface.
- We prove that if the bulk and surface reaction-diffusion systems have equal diffusion coefficients (i.e. $d_\Omega = d_\Gamma = 1$), no patterns form.
- In contrast to autonomous systems of coupled bulk-surface reaction-diffusion equations, in the presence of domain growth, reaction-kinetics of the form *short-range inhibition, long-range activation* in the bulk (i.e. $d_\Omega < 1$) and/or on the surface (i.e. $d_\Gamma < 1$), are capable of giving rise to pattern formation. Such kinetics can not give rise to patterning in the absence of growth (contraction) development.
- In contrast to autonomous systems of coupled bulk-surface reaction-diffusion equations, reaction-kinetics of the form *activator-activator* (during growth of the domain) or *inhibitior-inhibitor* (during domain contraction) are capable of giving rise only during growth development (both in the bulk and/or on the surface). Such kinetics can not give rise to patterning in the absence of growth (contraction) development.

Hence this article is structured as follows. In Section 2 we present the coupled bulk-surface reaction-diffusion system on evolving volumes with appropriate boundary conditions coupling the bulk and surface partial differential equations. As a first step for theoretical linear stability analysis, we propose a uniform isotropic evolution law for the evolving volumes .The main results of this article are presented in Section 3 where we derive Turing diffusion-driven instability conditions for the coupled system of bulk-surface reaction-diffusion equations on exponentially evolving volumes. Section 4 details the evolving bulk-surface finite element method applied to a coupled system of reaction-diffusion equations. To validate our theoretical findings, we present bulk-surface finite element numerical solutions in Section 5. In Section 6, we conclude and discuss the implications of our findings as well as articulating future challenges.

2. Coupled bulk-surface reaction-diffusion systems on evolving volumes

In this section we present a coupled system of bulk-surface reaction-diffusion equations (BSRDEs) posed in a three-dimensional evolving volume as well as on the evolving boundary surface enclosing the volume. We impose linear Robin-type boundary conditions on the bulk reaction-diffusion system while no boundary conditions are imposed on the surface reaction-diffusion system since the surface is closed.

2.1. A coupled system of bulk-surface reaction diffusion equations on evolving volumes

Let Ω_t be an evolving volume (whose interior is denoted the bulk) enclosed by a compact evolving hypersurface $\Gamma_t := \partial\Omega_t$ which is C^2. Also, let $I = [0, T]$ $(T > 0)$ be some time interval. Moreover, let $\boldsymbol{\nu}$ denote the unit outer normal to Γ_t, and let U be any open subset of $\mathbb{R}^m$ $(m \geq 2)$ containing Γ_t, then for any function u which is differentiable in U, we define the tangential gradient on Γ_t by, $\nabla_\Gamma u = \nabla u - (\nabla u \cdot \boldsymbol{\nu})\,\boldsymbol{\nu}$, where $\cdot$ denotes the regular dot product and ∇ denotes the regular gradient

in $\mathbb{R}^m$. The tangential gradient is the projection of the regular gradient onto the tangent plane, thus $\nabla_\Gamma u \cdot \boldsymbol{\nu} = 0$. The Laplace-Beltrami operator on the surface Γ_t is then defined to be the tangential divergence of the tangential gradient $\Delta_\Gamma u = \nabla_\Gamma \cdot \nabla_\Gamma u$. For a vector function $\boldsymbol{u} = (u_1, u_2, \ldots, u_m) \in \mathbb{R}^m$ the tangential divergence is defined by

$$\nabla_\Gamma \cdot \boldsymbol{u} = \nabla \cdot \boldsymbol{u} - \sum_{i=1}^{m} \Big(\nabla u_i \cdot \boldsymbol{\nu}\Big)\nu_i.$$

To proceed, we denote by $u : \Omega_t \times I \to \mathbb{R}$ and $v : \Omega_t \times I \to \mathbb{R}$ two chemical concentrations (species) that react and diffuse in Ω_t, and $r : \Gamma_t \times I \to \mathbb{R}$ and $s : \Gamma_t \times I \to \mathbb{R}$ be two chemical species residing only on the surface Γ_t which react and diffuse on the surface. Growth of the domain induces the material velocity (also known as the flow velocity) $\boldsymbol{v}$ which is generally modelled from experiments. In the absence of cross-diffusion and assuming that coupling is only through the reaction kinetics, we propose to study the following non-dimensionalised coupled system of BSRDEs

$$\begin{cases} \begin{cases} u_t + \nabla \cdot (\boldsymbol{v}u) = \Delta u + \gamma_\Omega f(u,v), \\ v_t + \nabla \cdot (\boldsymbol{v}v) = d_\Omega \Delta v + \gamma_\Omega g(u,v), \end{cases} & \text{in } \Omega_t \times (0,T], \\ \begin{cases} r_t + \nabla_\Gamma \cdot (\boldsymbol{v}r) = \Delta_\Gamma r + \gamma_\Gamma \Big(f(r,s) - h_1(u,v,r,s)\Big), \\ s_t + \nabla_\Gamma \cdot (\boldsymbol{v}s) = d_\Gamma \Delta_\Gamma s + \gamma_\Gamma \Big(g(r,s) - h_2(u,v,r,s)\Big), \end{cases} & \text{on } \Gamma_t \times (0,T], \end{cases} \tag{2.1}$$

with coupling boundary conditions

$$\begin{cases} (\boldsymbol{\nu} \cdot \nabla)\, u & = \gamma_\Gamma h_1(u,v,r,s), \\ d_\Omega\, (\boldsymbol{\nu} \cdot \nabla)\, v & = \gamma_\Gamma h_2(u,v,r,s), \end{cases} \quad \text{on } \Gamma_t \times (0,T]. \tag{2.2}$$

In the above, $\Delta = \frac{\partial^2}{\partial x^2} + \frac{\partial^2}{\partial y^2} + \frac{\partial^2}{\partial z^2}$ represents the Laplacian operator. d_Ω and d_Γ are a positive diffusion coefficients in the bulk and on the surface respectively, representing the ratio between u and v, and r and s, respectively. γ_Ω and γ_Γ represent the length scale parameters in the bulk and on the surface respectively. In this formulation, we assume that $f(\cdot,\cdot)$ and $g(\cdot,\cdot)$ are nonlinear reaction kinetics in the bulk and on the surface. $h_1(u,v,r,s)$ and $h_2(u,v,r,s)$ are reactions representing the coupling of the internal dynamics in the bulk Ω_t to the surface dynamics on the evolving surface Γ_t. As a first attempt, we will consider a more generalised form of linear coupling of the following nature [18]

$$h_1(u,v,r,s) = \alpha_1 r - \beta_1 u - \kappa_1 v, \tag{2.3}$$
$$h_2(u,v,r,s) = \alpha_2 s - \beta_2 u - \kappa_2 v, \tag{2.4}$$

where α_1, α_2, β_1, β_2, κ_1 and κ_2 are constant non-dimensionalised parameters. Initial conditions are given by the positive bounded functions $u_0(\boldsymbol{x})$, $v_0(\boldsymbol{x})$, $r_0(\boldsymbol{x})$ and $s_0(\boldsymbol{x})$.

Remark 2.1. In the absence of domain/volume growth, model system (2.1) reduces to a coupled system of bulk-surface reaction-diffusion system posed on stationary domains and volumes which was studied earlier (see [24, 26] for details).

Remark 2.2. The introduction of domain/volume growth in the model system of coupled bulk-surface partial differential equations results in two additional terms which are the convection term $\boldsymbol{v} \cdot \nabla u$ and the dilution or advection term $u(\nabla \cdot \boldsymbol{v})$.

2.1.1. Volume and surface evolution law

In many biological problems, volume and surface evolution is modelled from experimental observations and in general, the model equation for the flow velocity $\boldsymbol{v}$ is a complex nonlinear function involving the chemical species. In order to carry out some analytical studies, we assume that the volume and surface evolution law is governed by a uniform isotropic growth, independent of the chemical species, and is defined by

$$\boldsymbol{x}(t) = \rho(t)\boldsymbol{\xi}, \quad \text{with} \quad \boldsymbol{\xi} \in \Omega_0. \tag{2.5}$$

Under this form of growth, we can then define the flow velocity by

$$\boldsymbol{v} := \frac{d\boldsymbol{x}}{dt} = \dot{\rho}(t)\boldsymbol{\xi}. \tag{2.6}$$

As a result, it follows then that we can define

$$h(t) := \nabla \cdot \boldsymbol{v} = \frac{m\dot{\rho}(t)}{\rho(t)}, \quad \text{with} \quad m \geq 2. \tag{2.7}$$

Here m denotes the spatial dimension of Ω_t.

In the above framework, the growth function $\rho(t)$ is explicitly given and examples include linear, logistic and exponential as well as piece-wise continuous functions. Equally, $\rho(t)$ could be an interpolation function fitted to a discrete sequence of experimental observations. To proceed, we map for all time t, the model equations posed on evolving volumes and surfaces to models posed on stationary reference domains and surfaces as shown below [12, 21, 27].

2.1.2. Lagrangian transformation

Assuming spatially linear and isotropic evolution of the volume, we can write

$$\begin{cases} \begin{cases} \hat{u}(\boldsymbol{\xi},t) = u(\boldsymbol{x},t) = u(\rho(t)\boldsymbol{\xi},t), \\ \hat{v}(\boldsymbol{\xi},t) = v(\boldsymbol{x},t) = v(\rho(t)\boldsymbol{\xi},t), \end{cases} & \boldsymbol{\xi} \in \Omega_0,\ t \geq 0, \\ \begin{cases} \hat{r}(\boldsymbol{\xi},t) = r(\boldsymbol{x},t) = r(\rho(t)\boldsymbol{\xi},t), \\ \hat{s}(\boldsymbol{\xi},t) = s(\boldsymbol{x},t) = s(\rho(t)\boldsymbol{\xi},t), \end{cases} & \boldsymbol{\xi} \in \Gamma_0,\ t \geq 0. \end{cases} \tag{2.8}$$

It can be easily shown that the coupled bulk-surface reaction-diffusion system (2.1) simplifies to

$$\begin{cases} \begin{cases} \hat{u}_t + h(t)\hat{u} = \frac{1}{\rho^3(t)}\Delta\hat{u} + \gamma_\Omega f(\hat{u},\hat{v}), \\ \hat{v}_t + h(t)\hat{v} = \frac{d_\Omega}{\rho^3(t)}\Delta\hat{v} + \gamma_\Omega g(\hat{u},\hat{v}), \end{cases} & \text{in } \Omega_0 \times (0,T], \\ \begin{cases} \hat{r}_t + h(t)\hat{r} = \frac{1}{\rho^2(t)}\Delta_\Gamma\hat{r} + \gamma_\Gamma\Big(f(\hat{r},\hat{s}) - h_1(\hat{u},\hat{v},\hat{r},\hat{s})\Big), \\ \hat{s}_t + h(t)\hat{s} = \frac{d_\Gamma}{\rho^2(t)}\Delta_\Gamma\hat{s} + \gamma_\Gamma\Big(g(\hat{r},\hat{s}) - h_2(\hat{u},\hat{v},\hat{r},\hat{s})\Big), \end{cases} & \text{on } \Gamma_0 \times (0,T], \end{cases} \tag{2.9}$$

with coupling boundary conditions

$$\begin{cases} \frac{1}{\rho(t)}\left(\boldsymbol{\nu}\cdot\nabla\right)\hat{u} &= \gamma_\Gamma h_1(\hat{u},\hat{v},\hat{r},\hat{s}), \\ \frac{d_\Omega}{\rho(t)}\left(\boldsymbol{\nu}\cdot\nabla\right)\hat{v} &= \gamma_\Gamma h_2(\hat{u},\hat{v},\hat{r},\hat{s}), \end{cases} \quad \text{on } \Gamma_0 \times (0,T]. \tag{2.10}$$

2.1.3. Exponential evolution law

In this study, we will limit ourselves to studying only the case of an exponential evolution law of the system of coupled bulk-surface reaction-diffusion equations, we leave studies of other more complex evolution laws for future studies. It follows that given an exponential growth of the form

$$\rho(t) = e^{kt}, \quad \text{with} \quad k \in \mathbb{R}, \tag{2.11}$$

then

$$\begin{cases} h(t) = mk, \quad \text{if } \boldsymbol{\xi} \in \Omega_0, \\ \\ h(t) = (m-1)k, \quad \text{if } \boldsymbol{\xi} \in \Gamma_0. \end{cases} \tag{2.12}$$

Therefore, the coupled bulk-surface reaction-diffusion system (2.9) can now be posed in the following form, where we have dropped the ˆs for convenience's sake

$$\begin{cases} \begin{cases} u_t + mku = \frac{1}{\rho^3(t)}\Delta u + \gamma_\Omega f(u,v), \\ v_t + mkv = \frac{d_\Omega}{\rho^3(t)}\Delta v + \gamma_\Omega g(u,v), \end{cases} & \text{in } \Omega_0 \times (0,T], \\ \\ \begin{cases} r_t + (m-1)kr = \frac{1}{\rho^2(t)}\Delta_\Gamma r + \gamma_\Gamma\Big(f(r,s) - h_1(u,v,r,s)\Big), \\ s_t + (m-1)ks = \frac{d_\Gamma}{\rho^2(t)}\Delta_\Gamma s + \gamma_\Gamma\Big(g(r,s) - h_2(u,v,r,s)\Big), \end{cases} & \text{on } \Gamma_0 \times (0,T]. \end{cases} \tag{2.13}$$

Next we restrict our analysis to the well-known *activator-depleted* substrate model (also known as the Schnakenberg reaction kinetics) [10, 16, 34, 39, 43] since this model has a unique uniform steady state on stationary domains and volumes. Other kinetics can be studied in a similar fashion but with non-trivial uniform steady states. We note that by introducing domain growth, uniqueness of uniform steady state solutions for the *activator-depleted* model is not always guaranteed but depends crucially on the parameters that satisfy conditions for unique solutions for n-th order polynomials.

2.1.4. Activator-depleted reaction kinetics: An illustrative example

From now onwards, we restrict our analysis and simulations to the well-known *activator-depleted* substrate reaction model [10, 16, 34, 39, 43] also known as the Brusselator given by

$$f(u,v) = a - u + u^2\, v, \quad \text{and} \quad g(u,v) = b - u^2\, v, \tag{2.14}$$

where a and b are positive parameters. For analytical simplicity, we postulate the model system (2.13) in a more compact form given by

$$\begin{cases} \begin{cases} u_t = \frac{1}{\rho^3(t)}\Delta u + f_1(u,v,r,s), \\ v_t = \frac{d_\Omega}{\rho^3(t)}\Delta v + f_2(u,v,r,s), \end{cases} & \text{in } \Omega_0 \times (0,T], \\ \\ \begin{cases} r_t = \frac{1}{\rho^2(t)}\Delta_\Gamma r + f_3(u,v,r,s), \\ s_t = \frac{d_\Gamma}{\rho^2(t)}\Delta_\Gamma s + f_4(u,v,r,s), \end{cases} & \text{on } \Gamma_0 \times (0,T], \end{cases} \tag{2.15}$$

with coupling boundary conditions (2.10). In the above, we have defined appropriately

$$f_1(u,v,r,s) = \gamma_\Omega(a_1 - u + u^2 v) - mku, \tag{2.16}$$
$$f_2(u,v,r,s) = \gamma_\Omega(b_1 - u^2 v) - mkv, \tag{2.17}$$
$$f_3(u,v,r,s) = \gamma_\Gamma\big(a_2 - r + r^2 s - \alpha_1 r + \beta_1 u + \kappa_1 v\big) - (m-1)kr, \tag{2.18}$$
$$f_4(u,v,r,s) = \gamma_\Gamma\big(b_2 - r^2 s - \alpha_2 s + \beta_2 u + \kappa_2 v\big) - (m-1)ks. \tag{2.19}$$

Now, we are in a position to define the uniform steady states of the coupled bulk-surface reaction-diffusion system (2.15) with reaction-kinetics (2.16)-(2.19).

Definition 2.3 (Uniform steady states for an exponential growth)**.** A uniform steady state (u^*, v^*, r^*, s^*) is a constant solution of the coupled bulk-surface reaction-diffusion system (2.15) with reaction-kinetics (2.16)-(2.19), i.e. it satisfies that

$$f_1(u,v,r,s) = f_2(u,v,r,s) = f_3(u,v,r,s) = f_4(u,v,r,s) = 0$$

together with the boundary conditions

$$h_1(u,v,r,s) = 0 = h_2(u,v,r,s).$$

We state the existence theorem of the uniform steady states as follows.

Theorem 2.4. *(Existence of the uniform steady state for an exponential growth) There exists a uniform steady state* (u^*, v^*, r^*, s^*) *of the coupled bulk-surface reaction-diffusion system* (2.15) *with reaction-kinetics* (2.16)-(2.19) *satisfying the following conditions*

$$\begin{cases} v^* = \frac{\gamma_\Omega b_1}{\gamma_\Omega u^{*2} + mk}, \text{ where } u^* \text{ solves} \\ -\gamma_\Omega\left(\gamma_\Omega + mk\right)u^{*3} + \gamma_\Omega^2\left(a_1 + b_1\right)u^{*2} - mk\left(\gamma_\Omega + mk\right)u^* + a_1\gamma_\Omega mk = 0, \\ \\ s^* = \frac{\gamma_\Gamma b_2}{\gamma_\Gamma r^{*2} + (m-1)k}, \text{ where } r^* \text{ solves} \\ -\gamma_\Gamma\left(\gamma_\Gamma + (m-1)k\right)r^{*3} + \gamma_\Gamma^2\left(a_2 + b_2\right)r^{*2} - (m-1)k\left(\gamma_\Gamma + (m-1)k\right)r^* + a_2\gamma_\Gamma(m-1)k = 0, \end{cases}$$

for $m \geq 2,\ k \in \mathbb{R}$*, provided the following condition holds on the coupling boundary conditions*

$$\beta_1\kappa_1 - \beta_1\kappa_1 \neq 0. \tag{2.20}$$

Proof. The uniform steady state (u^*, v^*, r^*, s^*) solves the following system of non-algebraic equations

$$\gamma_\Omega(a_1 - u^* + u^{*2}v^*) - mku^* = 0, \tag{2.21}$$

$$\gamma_\Omega(b_1 - u^{*2}v^*) - mkv^* = 0, \tag{2.22}$$

$$\left(a_2 - r^* + r^{*2}s^* - \alpha_1 r^* + \beta_1 u^* + \kappa_1 v^*\right) - (m-1)kr^* = 0, \tag{2.23}$$

$$\gamma_\Gamma\left(b_2 - r^{*2}s^* - \alpha_2 s^* + \beta_2 u^* + \kappa_2 v^*\right) - (m-1)ks^* = 0. \tag{2.24}$$

as well as satisfying the coupling boundary conditions

$$\begin{bmatrix} \beta_1 & \kappa_1 \\ \beta_2 & \kappa_2 \end{bmatrix}\begin{bmatrix} u^* \\ v^* \end{bmatrix} = \begin{bmatrix} \alpha_1 r^* \\ \alpha_2 s^* \end{bmatrix}. \tag{2.25}$$

From (2.25), clearly u^* and v^* exists provided the determinant of the left matrix in (2.25) is non-singular, i.e. provided

$$\beta_1\kappa_2 - \beta_2\kappa_1 \neq 0.$$

If follows immediately from (2.22) that

$$v^* = \frac{\gamma_\Omega b_1}{\gamma_\Omega u^{*2} + mk} \tag{2.26}$$

where u^* is the solution of the nonlinear algebraic equation (2.21). Substituting v^* into (2.21) and simplifying leads to

$$-\gamma_\Omega\left(\gamma_\Omega + mk\right)u^{*3} + \gamma_\Omega^2\left(a_1 + b_1\right)u^{*2} - mk\left(\gamma_\Omega + mk\right)u^* + a_1\gamma_\Omega mk = 0 \tag{2.27}$$

as required. Similar calculations for the nonlinear algebraic system (2.23)-(2.24) leads to

$$s^* = \frac{\gamma_\Gamma b_2}{\gamma_\Gamma r^{*2} + (m-1)k} \tag{2.28}$$

where r^* is the solution of the cubic polynomial

$$-\gamma_\Gamma\left(\gamma_\Gamma + (m-1)k\right)r^{*3} + \gamma_\Gamma^2\left(a_2 + b_2\right)r^{*2} - (m-1)k\left(\gamma_\Gamma + (m-1)k\right)r^* + a_2\gamma_\Gamma(m-1)k = 0. \tag{2.29}$$

In the above, we have assumed uniformity of the bulk steady states on the surface boundary to yield the conditions

$$-\alpha_1 r^* + \beta_1 u^* + \kappa_1 v^* = 0, \tag{2.30}$$
$$-\alpha_2 s^* + \beta_2 u^* + \kappa_2 v^* = 0. \tag{2.31}$$

The existence of solutions to equations (2.30)-(2.31) leads immediately to equation (2.25). □

The existence of the uniform steady states (u^*, v^*, r^*, s^*) is intrinsically linked to the model parameters, in particular the following lemma holds.

Lemma 2.5. *The uniform steady state* (u^*, v^*, r^*, s^*) *of the coupled bulk-surface reaction-diffusion system* (2.15) *with reaction-kinetics* (2.16)-(2.19) *exists provided Theorem 2.4 holds and the coupling boundary parameter values must be chosen such that*

$$\begin{bmatrix} u^* \\ v^* \end{bmatrix} = \frac{1}{\beta_1\kappa_2 - \beta_2\kappa_1} \begin{bmatrix} \kappa_1 & -\kappa_2 \\ -\beta_1 & \beta_2 \end{bmatrix} \begin{bmatrix} \alpha_1 r^* \\ \alpha_2 s^* \end{bmatrix} \tag{2.32}$$

with $\beta_1\kappa_2 - \beta_2\kappa_1 \neq 0$.

The above lemma states the constraint conditions on the parameters in the coupling boundary conditions. These are not solutions to the uniform steady state. To proceed, we must study the existence and uniqueness of the solutions of the cubic polynomials (2.27) and (2.29). We will impose constraints on the model parameter values such that these polynomials yield unique solutions.

2.1.5. Existence and uniqueness of real solutions of cubic polynomials

Let us write the cubic polynomials (2.27) and (2.29) in more general terms:

$$c_3 w^3 + c_2 w^2 + c_1 w + c_0 = 0, \tag{2.33}$$

where

$$c_0 = a\gamma\mu k \tag{2.34}$$
$$c_1 = -\mu k\,(\gamma + \mu k) \tag{2.35}$$
$$c_2 = \gamma^2\,(a + b) \tag{2.36}$$
$$c_3 = -\gamma\,(\gamma + \mu k) \tag{2.37}$$

and $(w, \gamma, \mu, a, b) = (u^*, \gamma_\Omega, m, a_1, b_1)$ or $(r^*, \gamma_\Gamma, m-1, a_2, b_2)$. We are interested in the case that the cubic polynomial (2.33) has a single real root for each growth rate k. To this end the following theorem holds.

Theorem 2.6. *(Uniqueness of the uniform steady state for an exponential growth) The cubic polynomial* (2.33) *has a unique real root and two non-real complex conjugate roots if the discriminant of the cubic equation defined by*

$$\Delta = 18c_3c_2c_1c_0 - 4c_2^3c_0 + c_2^2c_1^2 - 4c_3c_1^3 - 27c_3^2c_0^2$$

is negative [13].

Define

$$W = w - \frac{c_2}{3c_3}. \tag{2.38}$$

Then (2.33) is equivalent to the reduced cubic in W:

$$W^3 + pW + q = 0, \tag{2.39}$$

where

$$p = \frac{3c_3c_1 - c_2^2}{3c_3^2}, \quad \text{and} \quad q = \frac{2c_2^3 - 9c_3c_2c_1 + 27c_3^2c_0}{27c_3^3}. \tag{2.40}$$

Then in the case where there is only one real root (i.e. when the condition in Theorem (2.6) is satisfied), the root W^* to (2.39) is given by

$$W^* = \begin{cases} -2\dfrac{|q|}{q}\sqrt{\dfrac{-p}{3}}\cosh\left(\dfrac{1}{3}\cosh^{-1}\left(-\dfrac{3|q|}{2p}\sqrt{-\dfrac{3}{p}}\right)\right) & \text{if } 4p^3 + 27q^2 > 0 \text{ and } p < 0, \\ -2\sqrt{\dfrac{p}{3}}\sinh\left(\dfrac{1}{3}\sinh^{-1}\left(\dfrac{3q}{2p}\sqrt{\dfrac{3}{p}}\right)\right) & \text{if } p > 0. \end{cases} \tag{2.41}$$

2.1.6. Homogeneous steady states with activator-depleted model

Below we compute the homogeneous steady state with *activator-depleted* kinetics in the bulk and on the surface. Here, we fix parameter values as follows:

$$a_1 = a_2 = 0.1, \ b_1 = b_2 = 0.9, \ \text{and } \gamma_\Omega = \gamma_\Gamma = 1$$

and take $m = 2$ and $m = 3$ (Figure 1) and vary the exponential growth rate k. With these parameter values, when there is no growth, $k = 0$, we recover the uniform steady state on stationary volumes given by [24]

$$(u^*, v^*, r^*, s^*)^T = \left(a_1 + b_1, \frac{b_1}{(a_1 + b_1)^2}, a_2 + b_2, \frac{b_2}{(a_2 + b_2)^2}\right)^T = (1.0, 0.9, 1.0, 0.9)^T$$

as shown in Figure 1 (when $k = 0$). Here we have imposed the following values for the coupling parameters: $\alpha_1 = \beta_1 = \frac{5}{12}$, $\alpha_2 = \kappa_2 = 5$, $\beta_2 = \kappa_1 = 0$. The equilibrium values v^* and s^* are given by equations (2.26) and (2.28), respectively. The equilibrium values u^* and r^* are obtained by solving (2.33). When solving (2.33) to find u^* and r^*, we fix a, b, γ and μ so that the only variable is k, the growth rate. In the computing algorithm, we then loop through different values of k and calculate the roots u^* and r^* using (2.41). We observe that for k small, u^* and r^* decrease monotonically, while v^* and s^* increase monotonically, reaching maxima for some growth rake k. As k gets larger and larger, the uniform steady states converge to a fixed stationary point that is constant for all k large. It must be noted that (u^*, v^*, r^*, s^*) are positive for all growth rates k and therefore for each fixed k, there exists a unique positive uniform steady state.

3. Linear stability analysis of the coupled bulk-surface reaction-diffusion systems

3.1. Linear stability in the absence of spatial variations

In this section we study diffusion-driven instability for the coupled bulk-surface reaction-diffusion system (2.15) with reaction-kinetics (2.16)-(2.19) for the case of the exponential growth. To proceed, we first consider the linear stability of the spatially uniform steady state in the absence of spatial variations. For convenience's sake, let us denote by $\boldsymbol{w} = \big(u,\ v,\ r,\ s\big)^T$, the vector of the species u, v, r and s. Furthermore, defining the vector $\boldsymbol{\xi}$ such that $|\xi_i| << 1$ for all $i = 1, 2, 3$ and 4, it follows that writing $\boldsymbol{w} = \boldsymbol{w}^* + \boldsymbol{\xi}$, the linearized system of coupled bulk-surface reaction-diffusion system can be posed as

$$\boldsymbol{w}_t = \boldsymbol{\xi}_t = \boldsymbol{J_F}\boldsymbol{\xi}, \tag{3.1}$$

where $\boldsymbol{J_F}$ represents the Jacobian matrix representing the first linear terms of the linearization process. Its entries are defined by

$$\boldsymbol{J_F} = \begin{pmatrix} \frac{\partial f_1}{\partial u} & \frac{\partial f_1}{\partial v} & \frac{\partial f_1}{\partial r} & \frac{\partial f_1}{\partial s} \\ \frac{\partial f_2}{\partial u} & \frac{\partial f_2}{\partial v} & \frac{\partial f_2}{\partial r} & \frac{\partial f_2}{\partial s} \\ \frac{\partial f_3}{\partial u} & \frac{\partial f_3}{\partial v} & \frac{\partial f_3}{\partial r} & \frac{\partial f_3}{\partial s} \\ \frac{\partial f_4}{\partial u} & \frac{\partial f_4}{\partial v} & \frac{\partial f_4}{\partial r} & \frac{\partial f_4}{\partial s} \end{pmatrix} := \begin{pmatrix} f_{1u} & f_{1v} & 0 & 0 \\ f_{2u} & f_{2v} & 0 & 0 \\ f_{3u} & f_{3v} & f_{3r} & f_{3s} \\ f_{4u} & f_{4v} & f_{4r} & f_{4s} \end{pmatrix} \tag{3.2}$$

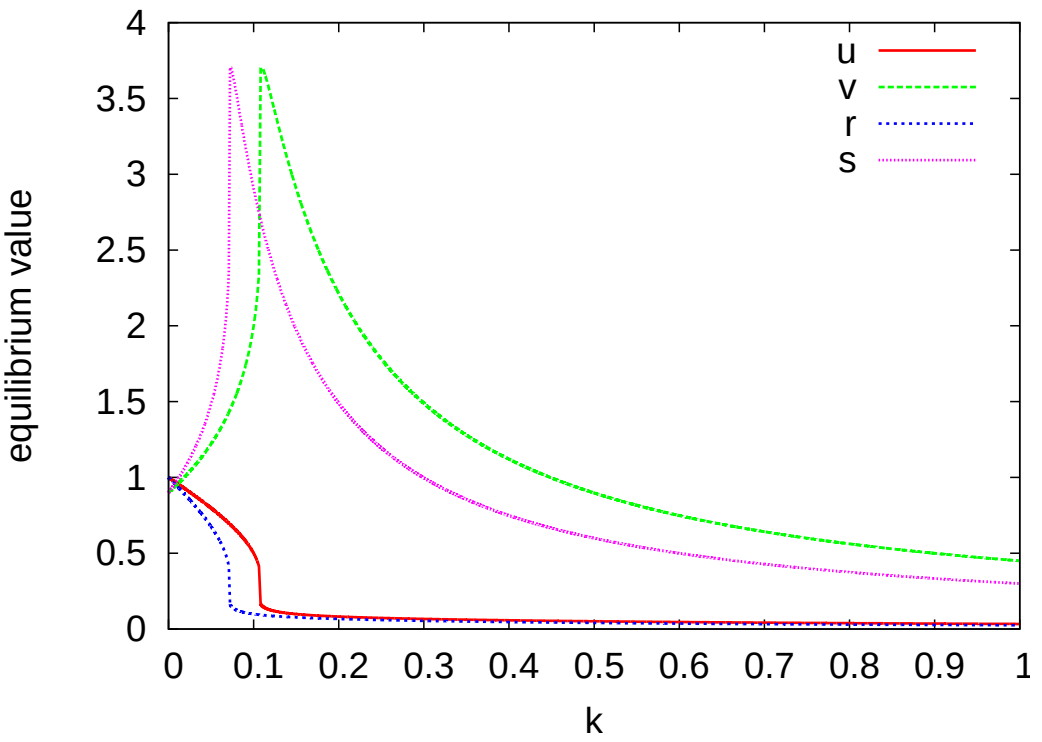

FIGURE 1. Plots of the uniform steady states as a function of the exponential growth rate k. Model parameter values are taken as $a_1 = a_2 = 0.1$, $b_1 = b_2 = 0.9$, and $\gamma_\Omega = \gamma_\Gamma = 1$. We fix the following values for the coupling parameters: $\alpha_1 = \beta_1 = \frac{5}{12}$, $\alpha_2 = \kappa_2 = 5$, $\beta_2 = \kappa_1 = 0$. (Colour figure online).

where by definition $f_{1u} := \frac{\partial f_1}{\partial u}$ represents a partial derivative of $f_1(u, v)$ with respect to u. We are looking for solutions to the system of linear ordinary differential equations (3.1) which are of the form $\boldsymbol{\xi} \propto e^{\lambda t}$. Substituting into (3.1), results in the following classical eigenvalue problem

$$\left|\lambda \boldsymbol{I} - \boldsymbol{J_F}\right| = 0, \tag{3.3}$$

where $\boldsymbol{I}$ is the identity matrix. Making appropriate substitutions and carrying out standard calculations we obtain the following dispersion relation for λ

$$\begin{aligned}\left|\lambda \boldsymbol{I} - \boldsymbol{J_F}\right| &= \begin{vmatrix} \lambda - f_{1u} & -f_{1v} & 0 & 0 \\ -f_{2u} & \lambda - f_{2v} & 0 & 0 \\ -f_{3u} & -f_{3v} & \lambda - f_{3r} & -f_{3s} \\ -f_{4u} & -f_{4v} & -f_{4r} & \lambda - f_{4s} \end{vmatrix} = 0, \\ \iff p(\lambda) &= \left(\lambda^2 - \mathrm{Tr}\left(\boldsymbol{J_F}\right)_\Omega \lambda + \mathrm{Det}\left(\boldsymbol{J_F}\right)_\Omega\right)\left(\lambda^2 - \mathrm{Tr}\left(\boldsymbol{J_F}\right)_\Gamma \lambda + \mathrm{Det}\left(\boldsymbol{J_F}\right)_\Gamma\right) = 0, \end{aligned} \tag{3.4}$$

where we have defined for convenience's sake

$$\left(\boldsymbol{J_F}\right)_\Omega := \begin{pmatrix} f_{1u} & f_{1v} \\ f_{2u} & f_{2v} \end{pmatrix} \quad \text{and} \quad \left(\boldsymbol{J_F}\right)_\Gamma := \begin{pmatrix} f_{3r} & f_{3s} \\ f_{4r} & f_{4s} \end{pmatrix} \tag{3.5}$$

the submatrices of $\boldsymbol{J_F}$ corresponding to the bulk and the surface reaction kinetics respectively. We can now define

$$\begin{aligned}&\mathrm{Tr}\left(\boldsymbol{J_F}\right) := f_{1u} + f_{2v} + f_{3r} + f_{4s}, \qquad \mathrm{Tr}\left(\boldsymbol{J_F}\right)_\Omega := f_{1u} + f_{2v}, \quad \mathrm{Tr}\left(\boldsymbol{J_F}\right)_\Gamma := f_{3r} + f_{4s},\\ &\mathrm{Det}\left(\boldsymbol{J_F}\right)_\Omega := f_{1u}f_{2v} - f_{1v}f_{2u}, \quad \text{and} \quad \mathrm{Det}\left(\boldsymbol{J_F}\right)_\Gamma := f_{3r}f_{4s} - f_{3s}f_{4r}.\end{aligned}$$

Theorem 3.1 (Necessary and sufficient conditions for $\mathrm{Re}(\lambda) < 0$)**.** *The necessary and sufficient conditions such that the zeros of the polynomial $p(\lambda)$ have $Re(\lambda) < 0$ are given by the following conditions*

$$Tr\left(\boldsymbol{J_F}\right)_\Omega < 0 \iff \gamma_\Omega(f_u + g_v) - 2mk < 0, \tag{3.6}$$

$$Tr\left(\boldsymbol{J_F}\right)_\Gamma < 0 \iff \gamma_\Gamma(f_r + g_s) - 2(m-1)k < 0, \tag{3.7}$$

$$Det\left(\boldsymbol{J_F}\right)_\Omega > 0 \iff \gamma_\Omega^2(f_u g_v - f_v g_u) - \gamma_\Omega(f_u + g_v)mk + m^2k^2 > 0, \tag{3.8}$$

$$Det\left(\boldsymbol{J_F}\right)_\Gamma > 0 \iff \gamma_\Gamma^2(f_r g_s - f_s g_r) - \gamma_\Gamma(f_r + g_s)(m-1)k + (m-1)^2k^2 > 0. \tag{3.9}$$

Proof. From the dispersion relation (3.4) it follows that

$$\left(\lambda^2 - \mathrm{Tr}\left(\boldsymbol{J_F}\right)_\Omega \lambda + \mathrm{Det}\left(\boldsymbol{J_F}\right)_\Omega\right)\left(\lambda^2 - \mathrm{Tr}\left(\boldsymbol{J_F}\right)_\Gamma \lambda + \mathrm{Det}\left(\boldsymbol{J_F}\right)_\Gamma\right) = 0 \tag{3.10}$$

if and only if

$$\lambda^2 - \mathrm{Tr}\left(\boldsymbol{J_F}\right)_\Omega \lambda + \mathrm{Det}\left(\boldsymbol{J_F}\right)_\Omega = 0 \tag{3.11}$$

or

$$\lambda^2 - \mathrm{Tr}\left(\boldsymbol{J_F}\right)_\Gamma \lambda + \mathrm{Det}\left(\boldsymbol{J_F}\right)_\Gamma = 0. \tag{3.12}$$

Solving (3.11) and (3.12) we obtain the following eigenvalues

$$\lambda_{1,2} = \frac{\mathrm{Tr}\left(\boldsymbol{J_F}\right)_\Omega \pm \sqrt{\mathrm{Tr}\left(\boldsymbol{J_F}\right)_\Omega^2 - 4\mathrm{Det}\left(\boldsymbol{J_F}\right)_\Omega}}{2}, \tag{3.13}$$

and

$$\lambda_{3,4} = \frac{\mathrm{Tr}\left(\boldsymbol{J_F}\right)_\Gamma \pm \sqrt{\mathrm{Tr}\left(\boldsymbol{J_F}\right)_\Gamma^2 - 4\mathrm{Det}\left(\boldsymbol{J_F}\right)_\Gamma}}{2}. \tag{3.14}$$

Clearly, it follows that

$$\mathrm{Re}(\lambda_{1,2}) < 0 \iff \mathrm{Tr}\left(\boldsymbol{J_F}\right)_\Omega < 0 \quad \text{and} \quad \mathrm{Det}\left(\boldsymbol{J_F}\right)_\Omega > 0. \tag{3.15}$$

Similarly

$$\mathrm{Re}(\lambda_{3,4}) < 0 \iff \mathrm{Tr}\left(\boldsymbol{J_F}\right)_\Gamma < 0 \quad \text{and} \quad \mathrm{Det}\left(\boldsymbol{J_F}\right)_\Gamma > 0. \tag{3.16}$$

This completes the proof. □

3.2. Linear stability analysis in the presence of spatial variations

Next we introduce spatial variations and study under what conditions the uniform steady state is linearly unstable. We linearize around the uniform steady state by taking small spatially varying perturbations of the form

$$\boldsymbol{w}(\boldsymbol{x}, t) = \boldsymbol{w}^* + \epsilon\boldsymbol{\xi}(\boldsymbol{x}, t), \quad \text{with} \quad \epsilon << 1. \tag{3.17}$$

Substituting (3.17) into the coupled bulk-surface reaction-diffusion system (2.15), with reaction-kinetics (2.16)-(2.19), we obtain a linearized system of partial differential equations of the form

$$\xi_{1t} = \frac{1}{\rho^3(t)}\Delta\xi_1 + f_{1u}\,\xi_1 + f_{1v}\,\xi_2, \tag{3.18}$$

$$\xi_{2t} = \frac{d_\Omega}{\rho^3(t)}\Delta\xi_2 + f_{2u}\,\xi_1 + f_{2v}\,\xi_2, \tag{3.19}$$

$$\xi_{3t} = \frac{1}{\rho^2(t)}\Delta_\Gamma\xi_3 + f_{3u}\,\xi_1 + f_{3v}\,\xi_2 + f_{3r}\,\xi_3 + f_{3s}\,\xi_4, \tag{3.20}$$

$$\xi_{4t} = \frac{d_\Gamma}{\rho^2(t)}\Delta_\Gamma\xi_4 + f_{4u}\,\xi_1 + f_{4v}\,\xi_2 + f_{4r}\,\xi_3 + f_{4s}\,\xi_4, \tag{3.21}$$

with linearised boundary conditions

$$\frac{1}{\rho(t)}\frac{\partial\xi_1}{\partial\nu} = \gamma_\Gamma\Big(h_{1u}\,\xi_1 + h_{1v}\,\xi_2 + h_{1r}\,\xi_3 + h_{1s}\,\xi_4\Big), \tag{3.22}$$

$$\frac{d_\Omega}{\rho(t)}\frac{\partial\xi_2}{\partial\nu} = \gamma_\Gamma\Big(h_{2u}\,\xi_1 + h_{2v}\,\xi_2 + h_{2r}\,\xi_3 + h_{2s}\,\xi_4\Big). \tag{3.23}$$

In order to proceed, we restrict our analysis to circular and spherical domains where we transform the cartesian coordinates into polar coordinates and exploit the method of separation of variables. Without loss of generality, we write the following eigenvalue problem in the bulk

$$\frac{1}{\rho^3(t)}\Delta\psi_{k_{l,m}}(r) = -k^2_{l,m}\psi_{k_{l,m}}(r), \quad 0 < r < 1, \tag{3.24}$$

where each ψ_k satisfies the boundary conditions (3.22) and (3.23). On the surface the eigenvalue problem is posed as

$$\frac{1}{\rho^2(t)}\Delta_\Gamma\phi(y) = -l(l+1)\phi(y), \quad y \in \Gamma. \tag{3.25}$$

Remark 3.2. For the case of circular and spherical domains, if $r = 1$, then $k^2_{l,m} = l(l+1)$.

Taking $x \in \mathbb{B}$, $y \in \Gamma$, then writing in polar coordinates $x = ry$, $r \in (0,1)$ we can define, for all $l \in \mathbb{N}_0$, $m \in \mathbb{Z}$, $|m| \leq l$, the following power series solutions [35, 36]

$$\xi_1(ry,t) = \sum u_{l,m}(t)\psi_{k_{l,m}}(r)\phi_{l,m}(y), \quad \xi_2(ry,t) = \sum v_{l,m}(t)\psi_{k_{l,m}}(r)\phi_{l,m}(y), \tag{3.26}$$

$$\xi_3(y,t) = \sum r_{l,m}(t)\phi_{l,m}(y), \quad \text{and} \quad \xi_4(y,t) = \sum s_{l,m}(t)\phi_{l,m}(y). \tag{3.27}$$

On the surface, substituting the power series solutions (3.27) into (3.20) and (3.21) we have

$$\begin{aligned}\frac{dr_{l,m}}{dt} &= -l(l+1)r_{l,m} + f_{3u}\,\xi_1 + f_{3v}\,\xi_2 + f_{3r}\,\xi_3 + f_{3s}\,\xi_4\\ &= -l(l+1)r_{l,m} + \Big(\gamma_\Gamma f_r - (m-1)k\Big)r_{l,m} + \gamma_\Gamma f_s\, s_{l,m}\\ &\quad - \gamma_\Gamma\Big(h_{1u}u_{l,m}\psi_{k_{l,m}}(1) + h_{1v}v_{l,m}\psi_{k_{l,m}}(1) + h_{1r}r_{l,m} + h_{1s}s_{l,m}\Big),\end{aligned} \tag{3.28}$$

$$\begin{aligned}\frac{ds_{l,m}}{dt} &= -d_\Gamma l(l+1)s_{l,m} + f_{4u}\,\xi_1 + f_{4v}\,\xi_2 + f_{4r}\,\xi_3 + f_{4s}\,\xi_4\\ &= -d_\Gamma l(l+1)s_{l,m} + \gamma_\Gamma g_r\, r_{l,m} + \Big(\gamma_\Gamma g_s - (m-1)k\Big)s_{l,m}\\ &\quad - \gamma_\Gamma\Big(h_{2u}u_{l,m}\psi_{k_{l,m}}(1) + h_{2v}v_{l,m}\psi_{k_{l,m}}(1) + h_{2r}r_{l,m} + h_{2s}s_{l,m}\Big).\end{aligned} \tag{3.29}$$

In the above, we have exploited the definitions of the reaction-kinetics as well as the boundary conditions.

Similarly, substituting the power series solutions (3.26) into the bulk equations (3.18) and (3.19) we obtain the following system of ordinary differential equations

$$\begin{aligned}\frac{du_{l,m}}{dt} &= -k_{l,m}^2 u_{l,m} + f_{1u}\,\xi_1 + f_{1v}\,\xi_2 \\ &= -k_{l,m}^2 u_{l,m} + \Big(\gamma_\Omega f_u - mk\Big)u_{l,m} + \gamma_\Omega f_v\, v_{l,m}, \qquad (3.30)\\ \frac{dv_{l,m}}{dt} &= -d_\Omega k_{l,m}^2 v_{l,m} + f_{2u}\,\xi_1 + f_{2v}\,\xi_2 \\ &= -d_\Omega k_{l,m}^2 v_{l,m} + \gamma_\Omega g_u\, u_{l,m} + \Big(\gamma_\Omega g_v - mk\Big)v_{l,m}. \qquad (3.31)\end{aligned}$$

Equations (3.30) and (3.31) are supplemented with boundary conditions

$$\frac{1}{\rho(t)}u_{l,m}\psi'_{k_{l,m}}(1) = \gamma_\Gamma\Big(h_{1u}u_{l,m}\psi_{k_{l,m}}(1) + h_{1v}v_{l,m}\psi_{k_{l,m}}(1) + h_{1r}r_{l,m} + h_{1s}s_{l,m}\Big), \qquad (3.32)$$

$$\frac{d_\Omega}{\rho(t)}v_{l,m}\psi'_{k_{l,m}}(1) = \gamma_\Gamma\Big(h_{2u}u_{l,m}\psi_{k_{l,m}}(1) + h_{2v}v_{l,m}\psi_{k_{l,m}}(1) + h_{2r}r_{l,m} + h_{2s}s_{l,m}\Big), \qquad (3.33)$$

where $\psi'_{k_{l,m}} := \frac{d\psi_{k_{l,m}}(r)}{dr}\Big|_{r=1}$. Writing

$$\big(u_{l,m}, v_{l,m}, r_{l,m}, s_{l,m},\big)^T = \big(u_{l,m}^0, v_{l,m}^0, r_{l,m}^0, s_{l,m}^0\big)^T e^{\int_0^t \lambda_{l,m}(\tau)d\tau},$$

and substituting into the system of ordinary differential equations (3.28)-(3.31), we obtain the following eigenvalue problem

$$\Big(\lambda_{l,m}(t)\boldsymbol{I} + \boldsymbol{M}\Big)\boldsymbol{\xi}_{l,m}^0 = \boldsymbol{0} \qquad (3.34)$$

where

$$\boldsymbol{M} = \begin{pmatrix} k_{l,m}^2 - \Big(\gamma_\Omega f_u - mk\Big) & -\gamma_\Omega f_v & 0 & 0 \\ -\gamma_\Omega g_u & d_\Omega k_{l,m}^2 - \Big(\gamma_\Omega g_v - mk\Big) & 0 & 0 \\ \frac{1}{\rho(t)}\psi'_{k_{l,m}}(1) & 0 & l(l+1) - \Big(\gamma_\Gamma f_r - (m-1)k\Big) & -\gamma_\Gamma f_s \\ 0 & \frac{d_\Omega}{\rho(t)}\psi'_{k_{l,m}}(1) & -\gamma_\Gamma g_r & d_\Gamma l(l+1) - \Big(\gamma_\Gamma g_s - (m-1)k\Big) \end{pmatrix},$$

and

$$\boldsymbol{\xi}_{l,m}^0 = \big(u_{l,m}^0, v_{l,m}^0, r_{l,m}^0, s_{l,m}^0\big)^T.$$

Note that the boundary conditions (3.32) and (3.33) have been applied appropriately to the surface linearised reaction-diffusion equations. Since

$$\big(u_{l,m}^0, v_{l,m}^0, r_{l,m}^0, s_{l,m}^0\big)^T \neq \big(0,0,0,0\big)^T,$$

it follows that the coefficient matrix must be singular, hence we require that

$$\Big|\lambda_{l,m}(t)\boldsymbol{I} + \boldsymbol{M}\Big| = 0.$$

Straight forward calculations show that the eigenvalue $\lambda_{l,m}$ solves the following dispersion relation written in compact form as

$$\Big(\lambda_{l,m}^2(t) + \mathrm{Tr}\,(\boldsymbol{M})_\Omega\,\lambda_{l,m}(t) + \mathrm{Det}\,(\boldsymbol{M})_\Omega\Big)\Big(\lambda_{l,m}^2(t) + \mathrm{Tr}\,(\boldsymbol{M})_\Gamma\,\lambda_{l,m}(t) + \mathrm{Det}\,(\boldsymbol{M})_\Gamma\Big) = 0, \qquad (3.35)$$

where we have defined conveniently

$$\begin{aligned}
\mathrm{Tr}(\boldsymbol{M})_{\Omega} &:= (d_{\Omega}+1)k_{l,m}^2 - \gamma_{\Omega}(f_u+g_v) + 2mk,\\
\mathrm{Tr}(\boldsymbol{M})_{\Gamma} &:= (d_{\Gamma}+1)l(l+1) - \gamma_{\Gamma}(f_r+g_s) + 2(m-1)k,\\
\mathrm{Det}(\boldsymbol{M})_{\Omega} &:= d_{\Omega}k_{l,m}^4 - \Big(\gamma_{\Omega}\left(d_{\Omega}f_u+g_v\right) - (d_{\Omega}+1)mk\Big)k_{l,m}^2 + \gamma_{\Omega}^2(f_ug_v - f_vg_u) - \gamma_{\Omega}(f_u+g_v)mk + m^2k^2,\\
\mathrm{Det}(\boldsymbol{M})_{\Gamma} &:= d_{\Gamma}l^2(l+1)^2 - \Big(\gamma_{\Gamma}\left(d_{\Gamma}f_r+g_s\right) - (d_{\Gamma}+1)(m-1)k\Big)l(l+1)\\
&\quad + \gamma_{\Gamma}^2(f_rg_s - f_sg_r) - \gamma_{\Gamma}(f_r+g_s)(m-1)k + (m-1)^2k^2.
\end{aligned}$$

Equality (3.35) holds true if and only if either

$$\lambda_{l,m}^2(t) + \mathrm{Tr}\left(\boldsymbol{M}\right)_{\Omega}\lambda_{l,m}(t) + \mathrm{Det}\left(\boldsymbol{M}\right)_{\Omega} = 0, \tag{3.36}$$

or

$$\lambda_{l,m}^2(t) + \mathrm{Tr}\left(\boldsymbol{M}\right)_{\Gamma}\lambda_{l,m}(t) + \mathrm{Det}\left(\boldsymbol{M}\right)_{\Gamma} = 0. \tag{3.37}$$

From here onwards, we drop the time-dependency in the eigenvalues assuming that these are implicitly functions of time. In the presence of diffusion, we require the emergence of spatial growth. In order for the uniform steady state $\boldsymbol{w}^*$ to be unstable we require that either

1. $\mathrm{Re}(\lambda_{l,m}(k_{l,m}^2)) > 0$ for some $k_{l,m}^2 > 0$,
   or
2. $\mathrm{Re}(\lambda_{l,m}(l(l+1))) > 0$ for some $l(l+1) > 0$,
   or
3. both.

Solving (3.36) (and similarly (3.37)) we obtain the eigenvalues

$$2\mathrm{Re}(\lambda_{l,m}(k_{l,m}^2)) = -\mathrm{Tr}\left(\boldsymbol{M}\right)_{\Omega} \pm \sqrt{\mathrm{Tr}^2\left(\boldsymbol{M}\right)_{\Omega} - 4\mathrm{Det}\left(\boldsymbol{M}\right)_{\Omega}}. \tag{3.38}$$

It follows then that $\mathrm{Re}(\lambda_{l,m}(k_{l,m}^2)) > 0$ for some $k_{l,m}^2 > 0$ if and only if the following conditions hold:

$$\begin{cases}
\mathrm{Tr}\left(\boldsymbol{M}\right)_{\Omega} < 0 \iff (d_{\Omega}+1)k_{l,m}^2 - \gamma_{\Omega}(f_u+g_v) + 2mk < 0, \quad \text{and}\\
\mathrm{Det}\left(\boldsymbol{M}\right)_{\Omega} > 0 \iff d_{\Omega}k_{l,m}^4 - \Big(\gamma_{\Omega}\left(d_{\Omega}f_u+g_v\right) - (d_{\Omega}+1)mk\Big)k_{l,m}^2 + \gamma_{\Omega}^2(f_ug_v - f_vg_u)\\
\qquad\qquad\qquad\qquad -\gamma_{\Omega}(f_u+g_v)mk + m^2k^2 > 0,
\end{cases} \tag{3.39}$$

or

$$\begin{cases}
\mathrm{Tr}\left(\boldsymbol{M}\right)_{\Omega} > 0 \iff (d_{\Omega}+1)k_{l,m}^2 - \gamma_{\Omega}(f_u+g_v) + 2mk > 0, \quad \text{and}\\
\mathrm{Det}\left(\boldsymbol{M}\right)_{\Omega} < 0 \iff d_{\Omega}k_{l,m}^4 - \Big(\gamma_{\Omega}\left(d_{\Omega}f_u+g_v\right) - (d_{\Omega}+1)mk\Big)k_{l,m}^2 + \gamma_{\Omega}^2(f_ug_v - f_vg_u)\\
\qquad\qquad\qquad\qquad -\gamma_{\Omega}(f_u+g_v)mk + m^2k^2 < 0.
\end{cases} \tag{3.40}$$

Similarly, on the surface, $\mathrm{Re}(\lambda_{l,m}(l(l+1))) > 0$ for some $l(l+1) > 0$ if and only the following conditions hold:

$$\begin{cases}
\mathrm{Tr}\left(\boldsymbol{M}\right)_{\Gamma} < 0 \iff (d_{\Gamma}+1)l(l+1) - \gamma_{\Gamma}(f_r+g_s) + 2(m-1)k < 0, \quad \text{and}\\
\mathrm{Det}\left(\boldsymbol{M}\right)_{\Gamma} > 0 \iff d_{\Gamma}l^2(l+1)^2 - \Big(\gamma_{\Gamma}\left(d_{\Gamma}f_r+g_s\right) - (d_{\Gamma}+1)(m-1)k\Big)l(l+1)\\
\qquad\qquad\qquad\qquad +\gamma_{\Gamma}^2(f_rg_s - f_sg_r) - \gamma_{\Gamma}(f_r+g_s)(m-1)k + (m-1)^2k^2 > 0,
\end{cases} \tag{3.41}$$

or

$$\begin{cases} \mathrm{Tr}\left(\boldsymbol{M}\right)_{\Gamma} > 0 \iff (d_{\Gamma}+1)l(l+1) - \gamma_{\Gamma}(f_r+g_s) + 2(m-1)k > 0, \quad \text{and} \\ \\ \mathrm{Det}\left(\boldsymbol{M}\right)_{\Gamma} < 0 \iff d_{\Gamma}l^2(l+1)^2 - \Big(\gamma_{\Gamma}\left(d_{\Gamma}f_r+g_s\right) - (d_{\Gamma}+1)(m-1)k\Big)l(l+1) \\ \qquad\qquad +\gamma_{\Gamma}^2(f_rg_s - f_sg_r) - \gamma_{\Gamma}(f_r+g_s)(m-1)k + (m-1)^2k^2 < 0. \end{cases} \tag{3.42}$$

From Theorem 3.1, conditions (3.39) and (3.41) are inadmissible since

$$\gamma_{\Omega}(f_u+g_v) - 2mk < 0 \Longrightarrow \mathrm{Tr}\left(\boldsymbol{M}\right)_{\Omega} > 0, \tag{3.43}$$

$$\gamma_{\Gamma}(f_r+g_s) - 2(m-1)k < 0 \Longrightarrow \mathrm{Tr}\left(\boldsymbol{M}\right)_{\Gamma} > 0. \tag{3.44}$$

The above conditions entail that only conditions (3.40) and (3.42) hold true and these imply that $\mathrm{Re}(\lambda_{l,m}(k_{l,m}^2)) > 0$ for some $k_{l,m}^2 > 0$ (and similarly $\mathrm{Re}(\lambda_{l,m}(l(l+1))) > 0$ for some $l(l+1) > 0$) provided that

$$\begin{aligned} \mathrm{Det}\left(\boldsymbol{M}\right)_{\Omega} < 0 \iff & d_{\Omega}k_{l,m}^4 - \Big(\gamma_{\Omega}\left(d_{\Omega}f_u+g_v\right) - (d_{\Omega}+1)mk\Big)k_{l,m}^2 \\ & + \gamma_{\Omega}^2(f_ug_v - f_vg_u) - \gamma_{\Omega}(f_u+g_v)mk + m^2k^2 < 0 \end{aligned} \tag{3.45}$$

and similarly on the surface we require that

$$\begin{aligned} \mathrm{Det}\left(\boldsymbol{M}\right)_{\Gamma} < 0 \iff & d_{\Gamma}l^2(l+1)^2 - \Big(\gamma_{\Gamma}\left(d_{\Gamma}f_r+g_s\right) - (d_{\Gamma}+1)(m-1)k\Big)l(l+1) \\ & + \gamma_{\Gamma}^2(f_rg_s - f_sg_r) - \gamma_{\Gamma}(f_r+g_s)(m-1)k + (m-1)^2k^2 < 0, \end{aligned} \tag{3.46}$$

respectively. Since d_{Ω} and d_{Γ} are strictly positive diffusion coefficients, and from Theorem 3.1

$$\begin{aligned} \gamma_{\Omega}^2(f_ug_v - f_vg_u) - \gamma_{\Omega}(f_u+g_v)mk + m^2k^2 > 0, \\ \gamma_{\Gamma}^2(f_rg_s - f_sg_r) - \gamma_{\Gamma}(f_r+g_s)(m-1)k + (m-1)^2k^2 > 0, \end{aligned}$$

then for $\mathrm{Det}\left(\boldsymbol{M}\right)_{\Omega} < 0$ (for some $k_{l,m}^2 > 0$) and $\mathrm{Det}\left(\boldsymbol{M}\right)_{\Gamma} < 0$ (for some $l(l+1) > 0$) we require that

$$d_{\Omega}f_u + g_v - (d_{\Omega}+1)mk > 0, \tag{3.47}$$

$$d_{\Gamma}f_r + g_s - (d_{\Gamma}+1)(m-1)k > 0. \tag{3.48}$$

We observe that $\mathrm{Det}\left(\boldsymbol{M}\right)_{\Omega}$ and $\mathrm{Det}\left(\boldsymbol{M}\right)_{\Gamma}$ are quadratic polynomials in k^2 and $l^2(l+1)^2$, respectively. The roots of these polynomials are given by, respectively

$$k_{l,m}{}_{\pm}^2 = \frac{\gamma_{\Omega}\left(d_{\Omega}f_u+g_v\right) - (d_{\Omega}+1)mk \pm \sqrt{\Big(\gamma_{\Omega}\left(d_{\Omega}f_u+g_v\right) - (d_{\Omega}+1)mk\Big)^2 - 4\mathrm{Det}\left(\boldsymbol{J_F}\right)_{\Omega}}}{2d_{\Omega}}$$

and

$$(l(l+1))_{\pm}^2 = \frac{\gamma_{\Gamma}\left(d_{\Gamma}f_r+g_s\right) - (d_{\Gamma}+1)(m-1)k \pm \sqrt{\Big(\gamma_{\Gamma}\left(d_{\Gamma}f_r+g_s\right) - (d_{\Gamma}+1)(m-1)k\Big)^2 - 4\mathrm{Det}\left(\boldsymbol{J_F}\right)_{\Gamma}}}{2d_{\Gamma}}.$$

Requiring real roots $k_{\pm}^2 > 0$ and $(l(l+1))_{\pm}^2 > 0$ implies that

$$\Big(\gamma_{\Omega}\left(d_{\Omega}f_u+g_v\right) - (d_{\Omega}+1)mk\Big)^2 - 4\mathrm{Det}\left(\boldsymbol{J_F}\right)_{\Omega} > 0, \tag{3.49}$$

and

$$\Big(\gamma_{\Gamma}\left(d_{\Gamma}f_r+g_s\right) - (d_{\Gamma}+1)(m-1)k\Big)^2 - 4\mathrm{Det}\left(\boldsymbol{J_F}\right)_{\Gamma} > 0, \tag{3.50}$$

respectively.

We summarise and state the necessary conditions for diffusion-driven instability on an exponentially growing volume in the following theorem.

Theorem 3.3. *The necessary conditions for a Turing diffusion-driven instability in the bulk and on the surface in the presence of spatially linear and isotropic exponentially growth as in system* (2.15) *with activator-depleted substrate kinetics* (2.14) *are given by*

$$\gamma_\Omega(f_u + g_v) - 2mk < 0, \tag{3.51}$$

$$\gamma_\Gamma(f_r + g_s) - 2(m-1)k < 0, \tag{3.52}$$

$$\gamma_\Omega^2(f_u g_v - f_v g_u) - \gamma_\Omega(f_u + g_v)mk + m^2k^2 > 0, \tag{3.53}$$

$$\gamma_\Gamma^2(f_r g_s - f_s g_r) - \gamma_\Gamma(f_r + g_s)(m-1)k + (m-1)^2k^2 > 0, \tag{3.54}$$

$$\gamma_\Omega\left(d_\Omega f_u + g_v\right) - (d_\Omega + 1)mk > 0, \tag{3.55}$$

$$\gamma_\Gamma\left(d_\Gamma f_r + g_s\right) - (d_\Gamma + 1)(m-1)k > 0, \tag{3.56}$$

$$\Big(\gamma_\Omega\left(d_\Omega f_u + g_v\right) - (d_\Omega + 1)mk\Big)^2 - 4\Big(\gamma_\Omega^2(f_u g_v - f_v g_u) - \gamma_\Omega(f_u + g_v)mk + m^2k^2\Big) > 0, \tag{3.57}$$

$$\Big(\gamma_\Gamma\left(d_\Gamma f_r + g_s\right) - (d_\Gamma + 1)(m-1)k\Big)^2 - 4\Big(\gamma_\Gamma^2(f_r g_s - f_s g_r) - \gamma_\Gamma(f_r + g_s)(m-1)k + (m-1)^2k^2\Big) > 0. \tag{3.58}$$

In the above, the subscripts u, v, r, s denote partial differentiation, with the Jacobian components f_u, f_v, f_r, f_s, g_u, g_v, g_r and g_s evaluated in terms of the uniform steady state (u^*, v^*, r^*, s^*) with $m \geq 2$.

Proof. The proof follows from the derivation above. □

3.3. Some remarks

Remark 3.4. Turing diffusion-driven instability can not occur for equal diffusion coefficients. Setting $d_\Omega = 1$ and $d_\Gamma = 1$ results in a contradiction between conditions (3.51) and (3.55), and (3.52) and (3.56) respectively.

Remark 3.5. Remark 3.4 implies that by selecting either $d_\Omega = 1$ in the bulk or $d_\Gamma = 1$ on the surface, the coupled bulk-surface system can give rise to diffusion-driven instability either only on the surface (for the case when $d_\Omega = 1$ in the bulk) or only in the bulk (for the case when $d_\Gamma = 1$ on the surface).

Remark 3.6. Suppose without loss of generality that u is an activator and v is an inhibitor for the generalised reaction-diffusion system (2.15). Thus $f_u > 0$ and $g_v < 0$. From inequalities (3.51) and (3.55), we require that

$$0 > \gamma_\Omega(f_u + g_v) - 2mk > (d_\Omega - 1)\left(2mk - \gamma_\Omega f_u\right), \text{ with } \gamma_\Omega > 0.$$

Therefore, it follows that $0 > (d_\Omega - 1)\left(2mk - \gamma_\Omega f_u\right)$; thus we can model new reaction kinetics that satisfy $0 < \gamma_\Omega f_u < 2mk$ requiring $0 < d_\Omega < 1$. Such a reaction kinetics will be of the from *short-range inhibition, long-range activation*, which is in contrast to the standard *long-range inhibition; short-range activation* kinetic models. Similarly, for the inequalities corresponding to the surface dynamics.

Remark 3.7. Similarly, let us assume that u is an activator in the reaction-diffusion system (2.15) so that $f_u > 0$. From inequality (3.51) we have

$$g_v < \left(\frac{2mk}{\gamma_\Omega} - f_u\right) < \frac{2mk}{\gamma_\Omega}.$$

Thus, we do not require $g_v < 0$, but that it suffices that g_v is bounded by the ratio between the growth terms and the scaling parameter γ_Ω. Therefore, it is plausible to have *activator-activator* kinetics (during growth of the domain) or *inhibitior-inhibitor* kinetics (during domain contraction). Similarly, for the inequalities corresponding to the surface dynamics. Such kinetics give rise to patterning only during growth (contraction) development.

3.4. Domain-induced parameter spaces

To validate our theoretical results, we plot parameter spaces defined by the inequalities (3.51)-(3.58) where we fix parameters $d_\Omega = 10$, $d_\Gamma = 10$, $\gamma_\Omega = 1$, $\gamma_\Gamma = 1$, and vary the growth rate k (see Figure 2. We plot parameter spaces as functions of the parameters of the (a_1, b_1) and (a_2, b_2) planes in the bulk and on the surface for illustrative purposes only, instead of plotting a four-dimensional parameter space for (a_1, b_1, a_2, b_2). It must be noted that inequalities (3.51)-(3.58) can be separated into Turing diffusion-driven inequalities in the bulk and on the surface respectively thereby allowing us to plot two-dimensional parameter spaces. For each case we plot spaces for $m = 2$ and $m = 3$ respectively (superimposed ontop of each each other). We note that the equilibrium values (u^*, v^*, r^*, s^*) are functions of (a_1, b_1) and (a_2, b_2) respectively, and therefore the values of the derivative in the inequalities (3.51)-(3.58), depend on the parameters (a_1, b_1) and (a_2, b_2). Thus the parameter spaces shown also indicate where there is a single real root for the equilibrium values (u^*, v^*) in (2.41) for the case of the bulk dynamics (similarly for (r^*, s^*) in the case of the surface dynamics). For $k << 1$ (in particular when k gets closer to zero), the

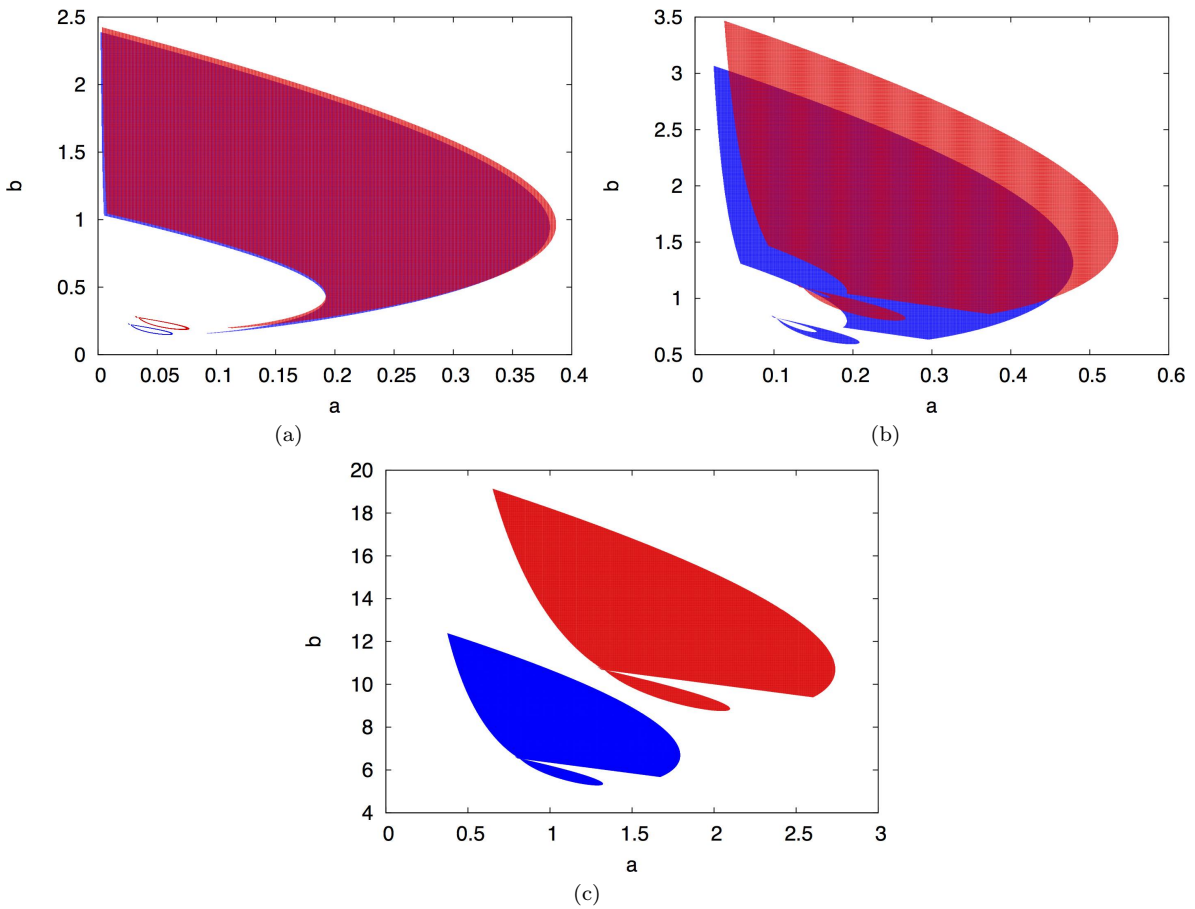

FIGURE 2. Plots of the parameter spaces defined by inequalities (3.51)-(3.58) where we fix $k = 0.001$ (a), $k = 0.1$ (b) and $k = 1$ (c). In all the plots, the parameter space in blue (bottom) corresponds to $m = 2$ and the parameter space in red (top) corresponds to $m = 3$. (Colour figure online).

parameter spaces become almost identical and these represent parameter spaces in the absence of domain growth. As k becomes larger and larger, the parameter spaces become more distinct and larger in size (including the circular subregions), reinforcing earlier results for standard reaction-diffusion systems on growing domains [21, 23, 25, 27]. The disconnected parameter spaces emerge due to the increase in the growth rate k as well as due to the dimension m.

4. The evolving bulk-surface finite element method

For ease of exposition, we will exploit the definition of the material derivative in deriving the weak formulation. If Γ_t is an hypersurface in $\mathbb{R}^3$ evolving in time t, according to a velocity field $\boldsymbol{v}$, we denote the material derivative of u by

$$\partial^\bullet u := u_t + \boldsymbol{v} \cdot \nabla u.$$

Theorem 4.1 (Reynolds Transport Theorem)**.** *Let $u(\boldsymbol{x}, t)$ be a scalar function defined on Ω_t and $\boldsymbol{v}$ be a flow velocity field then*

$$\frac{d}{dt} \int_{\boldsymbol{\Omega}_t} u \; d\boldsymbol{\Omega}_t = \int_{\boldsymbol{\Omega}_t} (\partial^\bullet u + u \nabla \cdot \boldsymbol{v}) \; d\boldsymbol{\Omega}_t. \tag{4.1}$$

A proof of this theorem can be found in [6, 20].

We can therefore rewrite the model system (2.1) in the form

$$\begin{cases} \begin{cases} \partial^\bullet u + u \nabla \cdot \boldsymbol{v} = \Delta u + \gamma_\Omega f(u, v), \\ \partial^\bullet v + v \nabla \cdot \boldsymbol{v} = d_\Omega \Delta v + \gamma_\Omega g(u, v), \end{cases} & \text{in } \Omega_t \times (0, T], \\ \\ \begin{cases} \partial^\bullet r + r \nabla_{\Gamma_t} \cdot \boldsymbol{v} = \Delta_{\Gamma_t} r + \gamma_\Gamma \Big(f(r, s) - h_1(u, v, r, s) \Big), \\ \partial^\bullet s + s \nabla_{\Gamma_t} \cdot \boldsymbol{v} = d_\Gamma \Delta_{\Gamma_t} s + \gamma_\Gamma \Big(g(r, s) - h_2(u, v, r, s) \Big), \end{cases} & \text{on } \Gamma_t \times (0, T]. \end{cases} \tag{4.2}$$

Now we are in a position to derive the weak variational form of the coupled bulk-surface reaction-diffusion system on evolving domains and surfaces as illustrated next. Here we exploit the definition of the material derivative as well as employing appropriately the Reynolds Transport Theorem 4.1. Note that the test function depends on space which implicitly depends on time, this is the key difference with models posed on stationary volumes.

4.1. The weak variational form

Let $\varphi(\boldsymbol{x}, t) \in H^1(\Omega_t)$ and $\psi(\boldsymbol{x}, t) \in H^1(\Gamma_t)$. Then, multiplying (4.2) by $\varphi(\boldsymbol{x}, t)$ and $\psi(\boldsymbol{x}, t)$, we seek to find $u, v \in L^2(0, t; H^1(\Omega_t))$ and $r, s \in L^2(0, t; H^1(\Gamma_t))$, such that

$$\begin{cases} \begin{cases} \int_{\Omega_t} \Big(\partial^\bullet (u\varphi) - u \partial^\bullet \varphi + u\varphi \nabla \cdot \boldsymbol{v} + \nabla u \cdot \nabla \varphi \Big) = \gamma_\Omega \int_{\Omega_t} (a_1 - u + u^2 v)\varphi \\ \qquad\qquad + \gamma_\Gamma \int_{\Gamma_t} (\alpha_1 r - \beta_1 u - \kappa_1 v)\varphi, \\ \int_{\Omega_t} \Big(\partial^\bullet (v\varphi) - v \partial^\bullet \varphi + v\varphi \nabla \cdot \boldsymbol{v} + d_\Omega \nabla v \cdot \nabla \varphi \Big) = \gamma_\Omega \int_{\Omega_t} (b_1 - u^2 v)\varphi \\ \qquad\qquad + \gamma_\Gamma \int_{\Gamma_t} (\alpha_2 s - \beta_2 u - \kappa_2 v)\varphi, \end{cases} & \boldsymbol{x} \text{ on } \Omega_t, \; t > 0, \\ \\ \begin{cases} \int_{\Gamma_t} \Big(\partial^\bullet (r\psi) - r \partial^\bullet \psi + r\psi \nabla_{\Gamma_t} \cdot \boldsymbol{v} + \nabla_{\Gamma_t} r \cdot \nabla_{\Gamma_t} \psi \Big) \\ \qquad = \gamma_\Gamma \int_{\Gamma_t} (a_2 - r + r^2 s - \alpha_1 r + \beta_1 u + \kappa_1 v)\psi, \\ \int_{\Gamma_t} \Big(\partial^\bullet (s\psi) - s \partial^\bullet \psi + s\psi \nabla_{\Gamma_t} \cdot \boldsymbol{v} + d_\Gamma \nabla_{\Gamma_t} s \cdot \nabla_{\Gamma_t} \psi \Big) \\ \qquad = \gamma_\Gamma \int_{\Gamma_t} (b_2 - r^2 s - \alpha_2 s + \beta_2 u + \kappa_2 v)\psi, \end{cases} & \boldsymbol{x} \text{ on } \Gamma_t, \; t > 0. \end{cases} \tag{4.3}$$

In the above, we have used Green's identities with the boundary conditions (2.2) to obtain the boundary integrals as well as exploiting the definition of the material derivative. Now calling upon the

Reynolds Transport Theorem [6], it can be easily shown that the weak variational form seeks to find $u, v \in L^2(0,t;H^1(\Omega_t))$ and $r, s \in L^2(0,t;H^1(\Gamma_t))$ solving

$$\begin{cases} \begin{cases} \frac{d}{dt}\int_{\Omega_t} u\varphi - \int_{\Omega_t} u\partial^\bullet\varphi + \int_{\Omega_t}\nabla u\cdot\nabla\varphi = \gamma_\Omega\int_{\Omega_t}(a_1 - u + u^2v)\varphi \\ \qquad\qquad +\gamma_\Gamma\int_{\Gamma_t}(\alpha_1 r - \beta_1 u - \kappa_1 v)\varphi, \\ \frac{d}{dt}\int_{\Omega_t} v\varphi - \int_{\Omega_t} v\partial^\bullet\varphi + d_\Omega\int_{\Omega_t}\nabla v\cdot\nabla\varphi = \gamma_\Omega\int_{\Omega_t}(b_1 - u^2v)\varphi \\ \qquad\qquad +\gamma_\Gamma\int_{\Gamma_t}(\alpha_2 s - \beta_2 u - \kappa_2 v)\varphi, \end{cases} \quad \boldsymbol{x} \text{ on } \Omega_t,\ t>0, \\ \\ \begin{cases} \frac{d}{dt}\int_{\Gamma_t} r\psi - \int_{\Gamma_t} r\partial^\bullet\psi + \int_{\Gamma_t}\nabla_{\Gamma_t} r\cdot\nabla_{\Gamma_t}\psi \\ \qquad = \gamma_\Gamma\int_{\Gamma_t}(a_2 - r + r^2 s - \alpha_1 r + \beta_1 u + \kappa_1 v)\psi, \\ \frac{d}{dt}\int_{\Gamma_t} s\psi - \int_{\Gamma_t} s\partial^\bullet\psi + d_\Gamma\int_{\Gamma_t}\nabla_{\Gamma_t} s\cdot\nabla_{\Gamma_t}\psi \\ \qquad = \gamma_\Gamma\int_{\Gamma_t}(b_2 - r^2 s - \alpha_2 s + \beta_2 u + \kappa_2 v)\psi, \end{cases} \quad \boldsymbol{x} \text{ on } \Gamma_t,\ t>0, \end{cases} \tag{4.4}$$

for all $\varphi \in H^1(\Omega_t)$ and for all $\psi \in H^1(\Gamma_t)$.

4.2. The evolving bulk-surface finite element method (EBSFEM)

4.2.1. Mesh generation on the initial domain volume

For finite element methods involving bulk and surface coupled dynamics, it is natural to define the surface discretisation as a collection of the faces of the elements of the bulk discretisation whose vertices lie on the surface. This implies that the surface discretisation is the trace of the bulk discretisation [14]. First we approximate Ω_t by Ω_t^h a bulk discretisation. Next we construct Γ_t^h to be the discretisation of the surface geometry Γ by defining $\Gamma_t^h = \Omega_t^h|_{\partial\Omega_t^h}$, i.e. the vertices of Γ_t^h are the same as those lying on the surface of Ω_t^h. In particular, we have $\partial\Omega_t^h = \Gamma_t^h$. The bulk discretisation induces the surface discretisation as illustrated in Figure 3. Throughout, we use hexahedral meshes for the bulk geometries which induce quadrilateral meshes for the surface geometries. For further details on techniques for generating bulk and surface discretisations with adaptivity, the reader is referred to the work of Köster *et al.*, (2008) [14]. During domain growth, the number of degrees of freedom and the mesh connectivity remains unchanged throughout.

4.2.2. The semi-discrete EBSFEM

First, we define the evolving bulk (V_t^h) and surface (S_t^h) finite element spaces that our evolving bulk-surface finite element method will be based on. For both cases, the finite element functions are defined to be continuous functions which are piece-wise linear with respect to the barycentric coordinates of the finite elements in 3-dimensions (for the bulk) and 2-dimensions (for the surface). To proceed, we approximate Ω_t by Ω_t^h, a discretised volume whose discretisation satisfy that $\Omega_t^h = \mathcal{B}_t^h = \bigcup_k B_k(t)$, where each $B_k(t)$ is a hexahedral prism. Similarly, we approximate Γ_t by Γ_t^h, a discretised surface whose vertices lie on $\Gamma(t)$, *i.e.*, $\Gamma_t^h = \mathcal{T}_t^h = \bigcup_l T_{l(t)}$, where each $T_l(t)$ is a quadrilateral. We can therefore define the evolving bulk finite element space

$$V_t^h := \left\{\varphi^h \in C^0(\Omega_t^h) :\ \varphi^h\big|_{B_k} \text{ is linear affine for each } B_k \in \mathcal{B}_t^h\right\}. \tag{4.5}$$

We assume Γ_t^h is smooth in time. For each t we define the evolving surface finite element space

$$S_t^h = \left\{\psi^h \in C^0(\Gamma_t^h) :\ \psi^h\big|_{T_l},\ \text{is linear affine for each } T_l \in \mathcal{T}_t^h\right\}. \tag{4.6}$$

For illustrative purposes, we consider the evolving surface finite element method and state without proof the transport property of the discrete material derivative. We will then derive the semi-discrete formulation for the evolving surface finite element method. The approach is identical in the case of the evolving bulk finite element element method (details omitted).

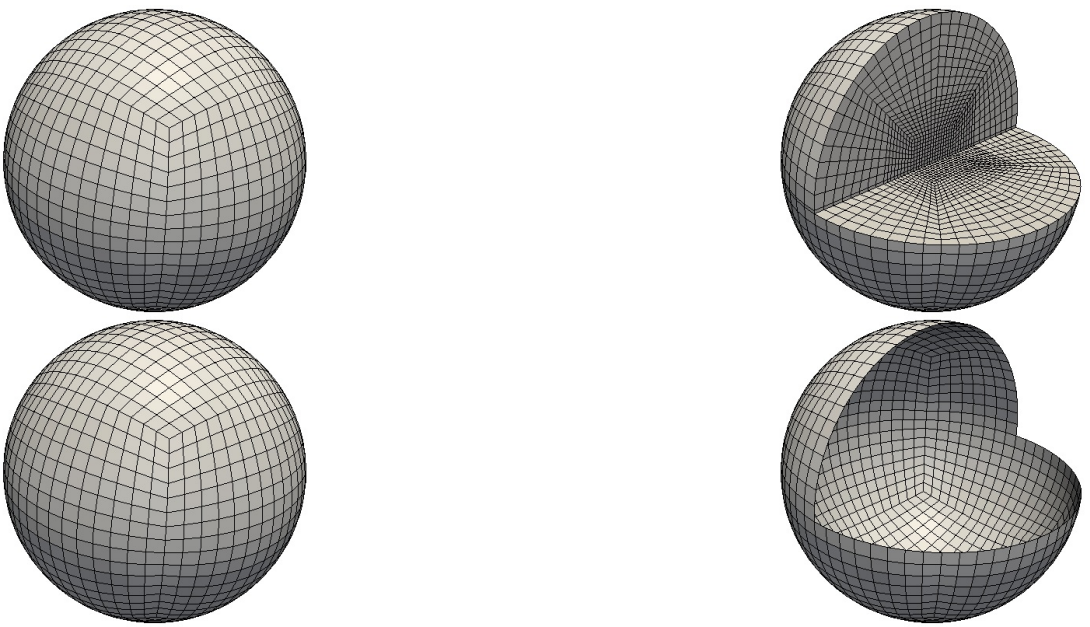

FIGURE 3. Example meshes for the bulk (top) and surface system (bottom). Part of the domain has been cut away and shown on the right to reveal some internal mesh structure (see [24] for details).

For the discretised surface, the diameter of the largest quadrilateral in the initial surface is denoted by h. We choose the vertices of the quadrilaterals to evolve with the material velocity such that

$$\dot{X}_j(t) = \boldsymbol{v}(X_j(t), t). \tag{4.7}$$

It is easy to note that $X_j(t)$ lies on Γ_t if $\boldsymbol{v}$ is the exact material velocity. For each $t \in [0,\, t_F]$ we denote by $\left\{\chi_j(\cdot,t)\right\}_{j=1}^{N_\Gamma}$ the moving nodal basis functions and by $X_j(t)$, $j = 1, \ldots, N_\Gamma$ the nodes. These functions will satisfy that

$$\chi_j(\cdot,t) \in C^0(\Gamma_t^h), \quad \chi_j(X_i(t),t) = \delta_{ij}, \quad \chi_j(\cdot,t)|_{T_l}\text{, is linear affine,}$$

and on $T_l \in \mathcal{T}_t^h$

$$\chi_j|_e = \lambda_k, \quad \text{for each } e \in \mathcal{T}_t^h,$$

where $k = k(T_l, j)$ and $(\lambda_1, \lambda_1, \lambda_3, \lambda_4)$ are the barycentric coordinates. On Γ_t^h we define the discrete material velocity

$$\boldsymbol{v}_h = \sum_{j=1}^{N_\Gamma} \dot{X}_j(t)\chi_j \tag{4.8}$$

and the discrete material derivative

$$\partial^\bullet \phi = \phi_t + \boldsymbol{v}_h \cdot \nabla\phi. \tag{4.9}$$

Proposition 4.2 (Transport Property)**.** *On Γ_t^h, for each $j = 1, \ldots, N_\Gamma$,*

$$\partial^\bullet \chi_j = 0$$

and for each $\phi = \sum_{j=1}^{N_\Gamma} \gamma_j(t)\chi_j \in S_t^h$ then $\partial^\bullet \phi = \sum_{j=1}^{N_\Gamma} \dot{\gamma}_j(t)\chi_j$.

Proof. It must be noted that the basis functions are functions of both space and time, the nodal spatial position for the discretised surface evolve according to the discrete material derivative and as a result the basis functions are simply transported with the flow. Hence their material derivative is zero. For a detailed proof, we refer the interested reader to consult the work of Dziuk [6]. □

Let $\{\varphi^i\}_{i=1}^{N_\Omega}$ and $\{\psi^i\}_{i=1}^{N_\Gamma}$ be two sets of piecewise bilinear shape functions on Ω_t^h and Γ_t^h respectively. Then these sets form a basis of V_t^h and S_t^h respectively. Thus, we seek approximations of $U(\cdot,t) \in V_t^h$ to u, $V(\cdot,t) \in V_t^h$ to v, $R(\cdot,t) \in S_t^h$ to r and $S(\cdot,t) \in S_t^h$ to s. Hence for each $t \in [0,\, t_F]$ there exist unique

$$\boldsymbol{u} = \left\{\alpha_u^1(t), \ldots, \alpha_u^{N_\Omega}(t)\right\}, \quad \boldsymbol{v} = \left\{\alpha_v^1(t), \ldots, \alpha_v^{N_\Omega}(t)\right\}, \tag{4.10}$$

$$\boldsymbol{r} = \left\{\alpha_r^1(t), \ldots, \alpha_r^{N_\Gamma}(t)\right\}, \quad \boldsymbol{s} = \left\{\alpha_s^1(t), \ldots, \alpha_s^{N_\Gamma}(t)\right\} \tag{4.11}$$

satisfying

$$U(\cdot,t) = \sum_{j=1}^{N_\Omega} \alpha_u^j(t)\varphi_u^j(\cdot,t), \qquad V(\cdot,t) = \sum_{j=1}^{N_\Omega} \alpha_v^j(t)\varphi_v^j(\cdot,t), \tag{4.12}$$

$$R(\cdot,t) = \sum_{j=1}^{N_\Gamma} \alpha_r^j(t)\psi_r^j(\cdot,t), \quad \text{and} \quad S(\cdot,t) = \sum_{j=1}^{N_\Gamma} \alpha_s^j(t)\psi_s^j(\cdot,t). \tag{4.13}$$

Substituting $U(\cdot,t)$, $V(\cdot,t)$, $R(\cdot,t)$, and $S(\cdot,t)$ in the coupled bulk-surface reaction-diffusion system (4.4), and taking into account the transport property of the basis functions φ_u^j, φ_v^j, ψ_r^j, and ψ_s^j, we obtain the following system expressed in matrix-vector form

$$\begin{cases} \begin{cases} \frac{d}{dt}\Big[\mathcal{M}_\Omega(t)\boldsymbol{u}\Big] + \mathcal{A}_\Omega(t)\boldsymbol{u} = \gamma_\Omega \boldsymbol{F}_1(t), \\ \\ \frac{d}{dt}\Big[\mathcal{M}_\Omega(t)\boldsymbol{v}\Big] + d_\Omega\mathcal{A}_\Omega(t)\boldsymbol{v} = \gamma_\Omega \boldsymbol{F}_2(t), \end{cases} \\ \\ \begin{cases} \frac{d}{dt}\Big[\mathcal{M}_\Gamma(t)\boldsymbol{r}\Big] + \mathcal{A}_\Gamma(t)\boldsymbol{r} = \gamma_\Gamma \boldsymbol{F}_3(t), \\ \\ \frac{d}{dt}\Big[\mathcal{M}_\Gamma(t)\boldsymbol{s}\Big] + d_\Gamma\mathcal{A}_\Gamma(t)\boldsymbol{s} = \gamma_\Gamma \boldsymbol{F}_4(t), \end{cases} \end{cases} \tag{4.14}$$

where $\mathcal{M}_\Omega(t)$ and $\mathcal{M}_\Gamma(t)$ are the evolving bulk- and surface-mass matrices defined by

$$\mathcal{M}_{\Omega jk}(t) = \int_{\Omega_t^h} \varphi^j \chi^k, \qquad \mathcal{M}_{\Gamma jk}(t) = \int_{\Gamma_t^h} \psi^j \chi^k,$$

$\mathcal{A}_\Omega(t)$ and $\mathcal{A}_\Gamma(t)$ are the evolving stiffness matrices defined by

$$\mathcal{A}_{\Omega jk}(t) = \int_{\Omega_t^h} \nabla\varphi^j \cdot \nabla\chi^k, \qquad \mathcal{A}_{\Gamma jk}(t) = \int_{\Gamma_t^h} \nabla_{\Gamma_h}\psi^j \cdot \nabla_{\Gamma_h}\chi^k$$

and $\boldsymbol{F}_i$, $i = 1, 2, 3, 4$, are the right hand side forcing vectors corresponding to the nonlinear terms, respectively. In the notation above for the basis functions, we have omitted the subscripts u, v, r and s respectively for notational simplicity. Similarly for the notation in the next section.

In particular, it can be shown that the space-discretised coupled bulk-surface reaction-diffusion system (4.14) for the case of the *activator-depleted* substrate kinetics (2.14) can be stated as follows:

$$\begin{cases} \begin{cases} \frac{d}{dt}\Big[\mathcal{M}_\Omega \boldsymbol{u}\Big] + \mathcal{A}_\Omega \boldsymbol{u} + \gamma_\Omega \mathcal{M}_\Omega \boldsymbol{u} - \gamma_\Omega B_{\boldsymbol{\varphi}}(\boldsymbol{u},\boldsymbol{v})\boldsymbol{u} \\ \qquad -\gamma_\Gamma\big(\alpha_1 M_{\varphi\psi}\boldsymbol{r} - \beta_1 M_{\varphi\varphi}\boldsymbol{u} - \kappa_1 M_{\varphi\varphi}\boldsymbol{v}\big) = \gamma_\Omega a_1 \mathbf{1}_{\boldsymbol{\varphi}}, \\ \frac{d}{dt}\Big[\mathcal{M}_\Omega \boldsymbol{v}\Big] + d_\Omega \mathcal{A}_\Omega \boldsymbol{v} + \gamma_\Omega B_{\boldsymbol{\varphi}}(\boldsymbol{u},\boldsymbol{u})\boldsymbol{v} \\ \qquad -\gamma_\Gamma\big(\alpha_2 M_{\varphi\psi}\boldsymbol{s} - \beta_2 M_{\varphi\varphi}\boldsymbol{u} - \kappa_2 M_{\varphi\varphi}\boldsymbol{v}\big) = \gamma_\Omega b_1 \mathbf{1}_{\boldsymbol{\varphi}}, \end{cases} & \text{in } \Omega_h \times (0,T], \\ \begin{cases} \frac{d}{dt}\Big[\mathcal{M}_\Gamma \boldsymbol{r}\Big] + \mathcal{A}_\Gamma \boldsymbol{r} + \gamma_\Gamma \mathcal{M}_\Gamma \boldsymbol{r} - \gamma_\Gamma B_{\boldsymbol{\psi}}(\boldsymbol{r},\boldsymbol{s})\boldsymbol{r} \\ \qquad +\gamma_\Gamma\big(\alpha_1 M_{\psi\psi}\boldsymbol{r} - \beta_1 M_{\psi\varphi}\boldsymbol{u} - \kappa_1 M_{\psi\varphi}\boldsymbol{v}\big) = \gamma_\Gamma a_2 \mathbf{1}_{\boldsymbol{\psi}}, \\ \frac{d}{dt}\Big[\mathcal{M}_\Gamma \boldsymbol{s}\Big] + d_\Gamma \mathcal{A}_\Gamma \boldsymbol{s} + \gamma_\Gamma B_{\boldsymbol{\psi}}(\boldsymbol{r},\boldsymbol{r})\boldsymbol{s} \\ \qquad +\gamma_\Gamma\big(\alpha_2 M_{\psi\psi}\boldsymbol{s} - \beta_2 M_{\psi\varphi}\boldsymbol{u} - \kappa_2 M_{\psi\varphi}\boldsymbol{v}\big) = \gamma_\Gamma b_2 \mathbf{1}_{\boldsymbol{\psi}}, \end{cases} & \text{on } \Gamma_h \times (0,T], \end{cases} \tag{4.15}$$

where $\mathbf{1}_\varphi$ is the column vector with j-th entry $\int_{\Omega_h} \varphi^j$. Given some vectors $\boldsymbol{a}$, $\boldsymbol{b}$ and $\boldsymbol{c}$, $B_{\boldsymbol{\varphi}}(\boldsymbol{a},\boldsymbol{b})$ is the matrix with entries

$$(B_{\boldsymbol{\varphi}})_{ij} = \int_{\Omega_h} (\boldsymbol{a}\cdot\boldsymbol{\varphi})(\boldsymbol{b}\cdot\boldsymbol{\varphi})\varphi^i\varphi^j \, d\boldsymbol{x}. \tag{4.16}$$

Similar quantities are defined for $\mathbf{1}_\psi$ and $B_{\boldsymbol{\psi}}$. The matrices $M_{\varphi\varphi}$, $M_{\varphi\psi}$, $M_{\psi\varphi}$ and $M_{\psi\psi}$ have entries

$$\begin{aligned} (M_{\varphi\varphi})^{ij} &= \int_{\Gamma_h} \varphi^i\varphi^j d\boldsymbol{x}, \qquad (M_{\varphi\psi})^{ij} = \int_{\Gamma_h} \varphi^i\psi^j d\boldsymbol{x}, \\ (M_{\psi\varphi})^{ij} &= \int_{\Gamma_h} \psi^i\varphi^j d\boldsymbol{x}, \quad \text{and} \quad (M_{\psi\psi})^{ij} = \int_{\Gamma_h} \psi^i\psi^j d\boldsymbol{x}. \end{aligned}$$

For further details, we refer the interested reader to [22, 26].

4.3. Time discretisation

We carry out the time-discretisation using the fractional-step θ method [22, 26]. This method is second order accurate when choosing $\theta = 1 - 1/\sqrt{2}$ and was the quickest in a selection of tested methods in a previous investigation [22]. For convergence, stability and performance of the numerical method, the reader is referred to [22]. For the time discretisation let T_m denote the maximum time of interest, τ denote the time step and J be a fixed nonnegative integer, then

$$\tau = \frac{T_m}{J} \quad \text{and} \quad t_k = k\tau, \quad k = 0, 1, 2, \ldots, J.$$

We denote the approximate solution at time t_k by $u_h^k = u_h(\cdot, t_k) = \boldsymbol{u}^k \cdot \boldsymbol{\varphi}$ and similarly for the other variables.

Following from (4.15), the fractional-step θ method is implemented as follows. Starting with the previous solution $(\boldsymbol{u}^n, \boldsymbol{v}^n, \boldsymbol{r}^n, \boldsymbol{s}^n)$, we first solve the coupled bulk-surface reaction-diffusion system (4.15) with the *activator-depleted* substrate kinetics (2.14) for the intermediate solution $(\boldsymbol{u}^{n+\theta}, \boldsymbol{v}^{n+\theta}, \boldsymbol{r}^{n+\theta}, \boldsymbol{s}^{n+\theta})$

$$\begin{cases} \frac{\mathcal{M}_\Omega^{n+\theta}\boldsymbol{u}^{n+\theta} - \mathcal{M}_\Omega^n \boldsymbol{u}^n}{\theta\tau} + \mathcal{A}_\Omega^{n+\theta}\boldsymbol{u}^{n+\theta} + \gamma_\Omega \mathcal{M}_\Omega^{n+\theta}\boldsymbol{u}^{n+\theta} \\ -\gamma_\Gamma\big(\alpha_1 M_{\varphi\psi}^{n+\theta}\boldsymbol{r}^{n+\theta} - \beta_1 M_{\varphi\varphi}^{n+\theta}\boldsymbol{u}^{n+\theta} - \kappa_1 M_{\varphi\varphi}^{n+\theta}\boldsymbol{v}^{n+\theta}\big) = \gamma_\Omega a_1 \mathbf{1}_\varphi^n + \gamma_\Omega B_{\boldsymbol{\varphi}}^n(\boldsymbol{u}^n,\boldsymbol{v}^n)\boldsymbol{u}^n, \\ \\ \frac{\mathcal{M}_\Omega^{n+\theta}\boldsymbol{v}^{n+\theta} - \mathcal{M}_\Omega^n \boldsymbol{v}^n}{\theta\tau} + d_\Omega \mathcal{A}_\Omega^{n+\theta}\boldsymbol{v}^{n+\theta} \\ -\gamma_\Gamma\big(\alpha_2 M_{\varphi\psi}^{n+\theta}\boldsymbol{s}^{n+\theta} - \beta_2 M_{\varphi\varphi}^{n+\theta}\boldsymbol{u}^{n+\theta} - \kappa_2 M_{\varphi\varphi}^{n+\theta}\boldsymbol{v}^{n+\theta}\big) = \gamma_\Omega b_1 \mathbf{1}_\varphi^n - \gamma_\Omega B_{\boldsymbol{\varphi}}^n(\boldsymbol{u}^n,\boldsymbol{u}^n)\boldsymbol{v}^n, \end{cases}$$

in the bulk and

$$\begin{cases} \frac{\mathcal{M}_\Gamma^{n+\theta}\boldsymbol{r}^{n+\theta}-\mathcal{M}_\Gamma^n\boldsymbol{r}^n}{\theta\tau}+\mathcal{A}_\Gamma^{n+\theta}\boldsymbol{r}^{n+\theta}+\gamma_\Gamma\mathcal{M}_\Gamma^{n+\theta}\boldsymbol{r}^{n+\theta} \\ +\gamma_\Gamma\big(\alpha_1 M_{\psi\psi}^{n+\theta}\boldsymbol{r}^{n+\theta}-\beta_1 M_{\psi\varphi}^{n+\theta}\boldsymbol{u}^{n+\theta}-\kappa_1 M_{\psi\varphi}^{n+\theta}\boldsymbol{v}^{n+\theta}\big)=\gamma_\Gamma a_2\mathbf{1}_\psi^n+\gamma_\Gamma B_{\boldsymbol{\psi}}^n(\boldsymbol{r}^n,\boldsymbol{s}^n)\boldsymbol{r}^n, \\ \\ \frac{\mathcal{M}_\Gamma^{n+\theta}\boldsymbol{s}^{n+\theta}-\mathcal{M}_\Gamma^n\boldsymbol{s}^n}{\theta\tau}+d_\Gamma\mathcal{A}_\Gamma^{n+\theta}\boldsymbol{s}^{n+\theta} \\ +\gamma_\Gamma\big(\alpha_2 M_{\psi\psi}^{n+\theta}\boldsymbol{s}^{n+\theta}-\beta_2 M_{\psi\varphi}^{n+\theta}\boldsymbol{u}^{n+\theta}-\kappa_2 M_{\psi\varphi}^{n+\theta}\boldsymbol{v}^{n+\theta}\big)=\gamma_\Gamma b_2\mathbf{1}_\psi^n-\gamma_\Gamma B_{\boldsymbol{\psi}}^n(\boldsymbol{r}^n,\boldsymbol{r}^n)\boldsymbol{s}^n, \end{cases}$$

on the surface. For the second intermediate solution $(\boldsymbol{u}^{n+1-\theta},\boldsymbol{v}^{n+1-\theta},\boldsymbol{r}^{n+1-\theta},\boldsymbol{s}^{n+1-\theta})$ we solve

$$\begin{cases} \frac{\mathcal{M}_\Omega^{n+1-\theta}\boldsymbol{u}^{n+1-\theta}-\mathcal{M}_\Omega^{n+\theta}\boldsymbol{u}^{n+\theta}}{(1-2\theta)\tau}-\gamma_\Omega B_{\boldsymbol{\varphi}}^{n+1-\theta}(\boldsymbol{u}^{n+1-\theta},\boldsymbol{v}^{n+1-\theta})\boldsymbol{u}^{n+1-\theta}=\gamma_\Omega a_1\mathbf{1}_\varphi^{n+\theta} \\ -\mathcal{A}_\Omega^{n+\theta}\boldsymbol{u}^{n+\theta}-\gamma_\Omega\mathcal{M}_\Omega^{n+\theta}\boldsymbol{u}^{n+\theta}+\gamma_\Gamma\big(\alpha_1 M_{\varphi\psi}^{n+\theta}\boldsymbol{r}^{n+\theta}-\beta_1 M_{\varphi\varphi}^{n+\theta}\boldsymbol{u}^{n+\theta}-\kappa_1 M_{\varphi\varphi}{}^{n+\theta}\boldsymbol{v}^{n+\theta}\big) \\ \frac{\mathcal{M}_\Omega^{n+1-\theta}\boldsymbol{v}^{n+1-\theta}-\mathcal{M}_\Omega^{n+\theta}\boldsymbol{v}^{n+\theta}}{(1-2\theta)\tau}+\gamma_\Omega B_{\boldsymbol{\varphi}}^{n+1-\theta}(\boldsymbol{u}^{n+1-\theta},\boldsymbol{u}^{n+1-\theta})\boldsymbol{v}^{n+1-\theta}=\gamma_\Omega b_1\mathbf{1}_\varphi^{n+\theta} \\ -d_\Omega\mathcal{A}_\Omega^{n+\theta}\boldsymbol{v}^{n+\theta}+\gamma_\Gamma\big(\alpha_2 M_{\varphi\psi}^{n+\theta}\boldsymbol{s}^{n+\theta}-\beta_2 M_{\varphi\varphi}^{n+\theta}\boldsymbol{u}^{n+\theta}-\kappa_2 M_{\varphi\varphi}^{n+\theta}\boldsymbol{v}^{n+\theta}\big), \end{cases} \tag{4.17}$$

in the bulk and

$$\begin{cases} \frac{\mathcal{M}_\Gamma^{n+1-\theta}\boldsymbol{r}^{n+1-\theta}-\mathcal{M}_\Gamma^{n+\theta}\boldsymbol{r}^{n+\theta}}{(1-2\theta)\tau}-\gamma_\Gamma B_{\boldsymbol{\psi}}^{n+1-\theta}(\boldsymbol{r}^{n+1-\theta},\boldsymbol{s}^{n+1-\theta})\boldsymbol{r}^{n+1-\theta}=\gamma_\Gamma a_2\mathbf{1}_\psi^{n+\theta} \\ -\mathcal{A}_\Gamma^{n+\theta}\boldsymbol{r}^{n+\theta}-\gamma_\Gamma\mathcal{M}_\Gamma^{n+\theta}\boldsymbol{r}^{n+\theta}-\gamma_\Gamma\big(\alpha_1 M_{\psi\psi}^{n+\theta}\boldsymbol{r}^{n+\theta}-\beta_1 M_{\psi\varphi}^{n+\theta}\boldsymbol{u}^{n+\theta}-\kappa_1 M_{\psi\varphi}^{n+\theta}\boldsymbol{v}^{n+\theta}\big), \\ \frac{\mathcal{M}_\Gamma^{n+1-\theta}\boldsymbol{s}^{n+1-\theta}-\mathcal{M}_\Gamma^{n+\theta}\boldsymbol{s}^{n+\theta}}{(1-2\theta)\tau}+\gamma_\Gamma B_{\boldsymbol{\psi}}^{n+1-\theta}(\boldsymbol{r}^{n+1-\theta},\boldsymbol{r}^{n+1-\theta})\boldsymbol{s}^{n+1-\theta}=\gamma_\Gamma b_2\mathbf{1}_\psi^{n+\theta} \\ -d_\Gamma\mathcal{A}_\Gamma^{n+\theta}\boldsymbol{s}^{n+\theta}-\gamma_\Gamma\big(\alpha_2 M_{\psi\psi}^{n+\theta}\boldsymbol{s}^{n+\theta}-\beta_2 M_{\psi\varphi}^{n+\theta}\boldsymbol{u}^{n+\theta}-\kappa_2 M_{\psi\varphi}^{n+\theta}\boldsymbol{v}^{n+\theta}\big), \end{cases} \tag{4.18}$$

on the surface. Finally for the new solution $(\boldsymbol{u}^{n+1},\boldsymbol{v}^{n+1},\boldsymbol{r}^{n+1},\boldsymbol{s}^{n+1})$ we solve

$$\begin{cases} \frac{\mathcal{M}_\Omega^{n+1}\boldsymbol{u}^{n+1}-\mathcal{M}_\Omega^{n+1-\theta}\boldsymbol{u}^{n+1-\theta}}{\theta\tau}+\mathcal{A}_\Omega^{n+1}\boldsymbol{u}^{n+1}+\gamma_\Omega\mathcal{M}_\Omega^{n+1}\boldsymbol{u}^{n+1} \\ \qquad -\gamma_\Gamma\big(\alpha_1 M_{\varphi\psi}^{n+1}\boldsymbol{r}^{n+1}-\beta_1 M_{\varphi\varphi}^{n+1}\boldsymbol{u}^{n+1}-\kappa_1 M_{\varphi\varphi}^{n+1}\boldsymbol{v}^{n+1}\big) \\ \qquad\qquad =\gamma_\Omega a_1\mathbf{1}_\varphi^{n+1-\theta}+\gamma_\Omega B_{\boldsymbol{\varphi}}^{n+1-\theta}(\boldsymbol{u}^{n+1-\theta},\boldsymbol{v}^{n+1-\theta})\boldsymbol{u}^{n+1-\theta}, \\ \frac{\mathcal{M}_\Omega^{n+1}\boldsymbol{v}^{n+1}-\mathcal{M}_\Omega^{n+1-\theta}\boldsymbol{v}^{n+1-\theta}}{\theta\tau}+d_\Omega\mathcal{A}_\Omega^{n+1}\boldsymbol{v}^{n+1} \\ \qquad -\gamma_\Gamma\big(\alpha_2 M_{\varphi\psi}^{n+1}\boldsymbol{s}^{n+1}-\beta_2 M_{\varphi\varphi}^{n+1}\boldsymbol{u}^{n+1}-\kappa_2 M_{\varphi\varphi}^{n+1}\boldsymbol{v}^{n+1}\big) \\ \qquad\qquad =\gamma_\Omega b_1\mathbf{1}_\varphi^{n+1-\theta}-\gamma_\Omega B_{\boldsymbol{\varphi}}^{n+1-\theta}(\boldsymbol{u}^{n+1-\theta},\boldsymbol{u}^{n+1-\theta})\boldsymbol{v}^{n+1-\theta}, \end{cases}$$

in the bulk and

$$\begin{cases} \frac{\mathcal{M}_\Gamma^{n+1}\boldsymbol{r}^{n+1}-\mathcal{M}_\Gamma^{n+1-\theta}\boldsymbol{r}^{n+1-\theta}}{\theta\tau}+\mathcal{A}_\Gamma^{n+1}\boldsymbol{r}^{n+1}+\gamma_\Gamma\mathcal{M}_\Gamma^{n+1}\boldsymbol{r}^{n+1} \\ \qquad +\gamma_\Gamma\big(\alpha_1 M_{\psi\psi}^{n+1}\boldsymbol{r}^{n+1}-\beta_1 M_{\psi\varphi}^{n+1}\boldsymbol{u}^{n+1}-\kappa_1 M_{\psi\varphi}^{n+1}\boldsymbol{v}^{n+1}\big) \\ \qquad\qquad =\gamma_\Gamma a_2\mathbf{1}_\psi^{n+1-\theta}+\gamma_\Gamma B_{\boldsymbol{\psi}}^{n+1-\theta}(\boldsymbol{r}^{n+1-\theta},\boldsymbol{s}^{n+1-\theta})\boldsymbol{r}^{n+1-\theta}, \\ \frac{\mathcal{M}_\Gamma^{n+1}\boldsymbol{s}^{n+1}-\mathcal{M}_\Gamma^{n+1-\theta}\boldsymbol{s}^{n+1-\theta}}{\theta\tau}+d_\Gamma\mathcal{A}_\Gamma^{n+1}\boldsymbol{s}^{n+1} \\ \qquad +\gamma_\Gamma\big(\alpha_2 M_{\psi\psi}^{n+1}\boldsymbol{s}^{n+1}-\beta_2 M_{\psi\varphi}^{n+1}\boldsymbol{u}^{n+1}-\kappa_2 M_{\psi\varphi}^{n+1}\boldsymbol{v}^{n+1}\big) \\ \qquad\qquad =\gamma_\Gamma b_2\mathbf{1}_\psi^{n+1-\theta}-\gamma_\Gamma B_{\boldsymbol{\psi}}^{n+1-\theta}(\boldsymbol{r}^{n+1-\theta},\boldsymbol{r}^{n+1-\theta})\boldsymbol{s}^{n+1-\theta}, \end{cases}$$

on the surface. The presence of the B matrices on the left-hand side makes the system in the second step (4.17) and (4.18) nonlinear. The nonlinearities are solved using the iterative Newton method [22]. The linear system is then solved by use of the biconjugate gradient stabilized method, often abbreviated BiCGSTAB, which is an iterative numerical method developed for the numerical solution of nonsymmetric linear systems [22, 26, 38, 42].

Remark 4.3. It must be observed that for the fractional-step θ method above, the computational mesh is continuously evolving according to the exponential growth and all matrices are assembled at different discretised surfaces depending on the time-level n. The number of degrees of freedom and the mesh connectivity remains constant throughout domain growth. For further details on the implementation of the evolving (bulk) surface finite element method we refer the interested reader to [2, 6, 7, 23].

Remark 4.4 (Stability and convergence of the bulk-surface finite element method)**.** Detailed numerical analysis involving mesh and time-refinement as well as convergence of the bulk-surface finite element solver has been carried out in our previous study and we refer the interested reader to consult [22, 26] for further details.

5. Numerical experiments

5.1. Parameter values

For illustrative purposes we take the following parameter values

$$a_1 = a_2 = 0.1,\ b_1 = b_2 = 0.9,\ k = 0.01,\ \alpha_1 = \beta_1 = \frac{5}{12},\ \alpha_2 = \kappa_2 = 5,\ \beta_2 = \kappa_1 = 0.$$

We only present patterns corresponding to the chemical species u and r in the bulk and on the surface respectively. Those corresponding to v and s are 180 degrees out of phase to those of u and r and are therefore omitted. It must be noted however that this is not always the case in general, Robin-type boundary conditions may alter the structure of the solution profiles depending on the model parameter values and the coupling compatibility boundary parameters.

5.1.1. Simulations of the coupled system of BSRDEs with $(d_\Omega, d_\Gamma) = (20, 20),\ \gamma_\Omega = \gamma_\Gamma = 29,\ T_f = 30$

For our first example, we compute solutions for the coupled bulk-surface reaction-diffusion systems (2.1)-(2.14) with *activator-depleted* kinetics for $d_\Omega = 20$ in the bulk and $d_\Gamma = 20$ on the surface and scaling parameters $\gamma_\Omega = \gamma_\Gamma = 29$ and plot these as a sequences at times $t = 5$, $t = 15$, $t = 25$ and final time $T_f = 30$. The solutions are illustrated in Figure 4. We observe the formation of spot patterns as the sphere continues to evolve exponentially. For these scaling parameters, it is well known patterning will form since the initial length scale is sufficiently large enough to allow pattern to emerge. In our next example, we demonstrate the role of domain growth, by selecting much much smaller scaling parameters, patterning is only induced due to domain evolution.

5.1.2. Simulations of the coupled system of BSRDEs with $(d_\Omega, d_\Gamma) = (20, 20),\ \gamma_\Omega = \gamma_\Gamma = 1,\ T_f = 20$

In this example, we illustrate how domain growth induces pattering in the bulk and on the surface by taking $d_\Omega = 20$ in the bulk, $d_\Gamma = 20$ on the surface and scaling parameters $\gamma_\Omega = \gamma_\Gamma = 1$. For these scaling parameters, reaction-diffusion systems of this type do not give rise to Turing pattern on stationary volumes simply because the length scale is not large enough to allow for patterning [21,30,41]. However, by introducing domain growth, patterning emerges in the bulk and on the surface. Figure 5 shows pattern formation in the bulk and on the surface during an exponential growth of the sphere. Unlike in the previous example, in the bulk we take cross-sections to reveal patterns observed inside the bulk. For these parameter values (noting that $\gamma_\Omega = \gamma_\Gamma = 1$) we observe high concentration values of the solutions closer to and on the surface with lower values in the interior of the bulk. We also observe the emergence of patterns with small amplitudes on the surface during early growth development (compared to large amplitude solutions in the bulk) and this is due to the short time taken to terminate the solutions.

Remark 5.1. Due to the computational costs involved in solving these complex systems of coupled bulk-surface reaction-diffusion equations on evolving volumes, we have chosen to show only two sets of results for fixed diffusion parameter values $d_\Omega = 20$ in the bulk, $d_\Gamma = 20$ on the surface and variable scaling parameters $\gamma_\Omega = \gamma_\Gamma = 1,\ 29$, respectively. Other parameter variations can be simulated by taking

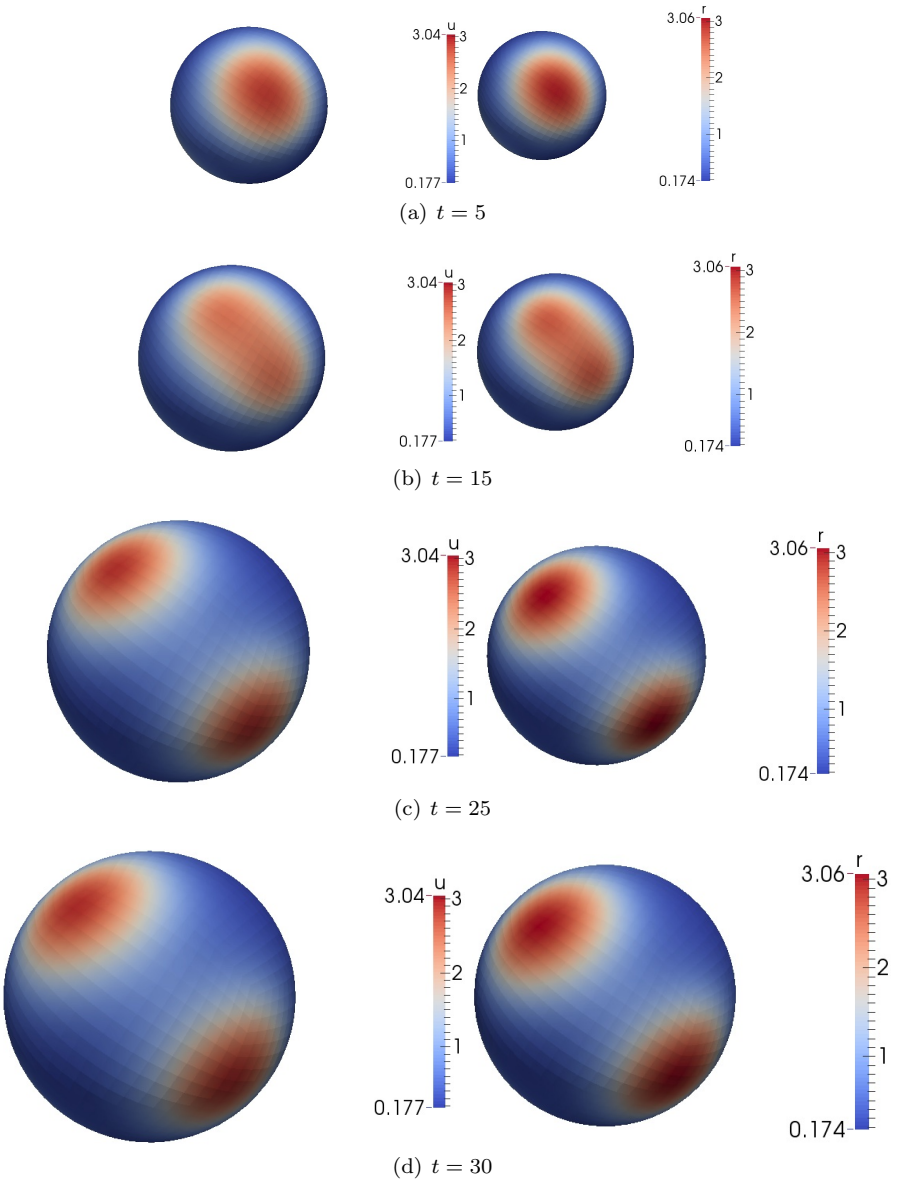

(a) $t = 5$

(b) $t = 15$

(c) $t = 25$

(d) $t = 30$

FIGURE 4. Numerical solutions corresponding to the coupled system of BSRDEs (2.1)-(2.14) with *activator-depleted* kinetics for $d_\Omega = 20$ in the bulk and $d_\Gamma = 20$ on the surface and scaling parameters $\gamma_\Omega = \gamma_\Gamma = 29$. Column 1: solutions in the bulk representing u and Columns 2: solutions on the surface representing r. We observe spot pattern formation in the bulk and on the surface. (Colour figure online).

different diffusion coefficients in the bulk and on the surface to generate a wide range of patterns either concentrated in the bulk or on the surface (results not shown). We refer the interested reader to see [24] for such pattern diversity albeit on stationary volumes. Our second example shows how domain growth enhances patterning for the case where no patterning will occur in the absence of domain growth. Taking larger values of γ_Ω in the bulk and γ_Γ on the surface results in the emergence of more complex patterns such as spots, stripes and circular as well as combinations of these (results not shown).

6. Conclusion

In this article we have presented a detailed stability analysis of a system of coupled bulk-surface reaction-diffusion equations with linear Robin-type boundary conditions on exponentially evolving volumes. A key result of our analysis is that we are able to derive the necessary conditions for diffusion-driven instability which are a substantial generalisation of Turing's conditions for patterning on stationary domains. Our theoretical results predict the formation of patterns either in the bulk or on the surface or both in the bulk and on the surface dependent on the model parameter values. Unlike the standard case, pattern generation no longer requires *long-range inhibition short-range activation* as a necessary mechanism for pattern formation. Other non-standard mechanisms such as *short-range inhibition long-range activation*, *activator-activator* (only during growth development) and *inhibitor-inhibitor* (only during growth contraction) are capable of giving rise to the emergence of spatial pattern formation only during growth (contraction) development. Such patterns depend crucially on the model parameter values as well as on appropriate reaction-kinetics. An example of an *activator-activator* reaction-diffusion model was presented in previous studies on growing domains (see [21, 40] for details and patterns generated); such a model is capable of giving rise to the formation of spatial structure only during growth development.

The modelling and computational framework we have developed in this article offers us a platform to study more complex systems of coupled bulk-surface reaction-diffusion equations with applications to cell motility and pattern formation. We envisage the following extensions of the current framework: to investigate the role of coupling boundary conditions for systems of coupled bulk-surface reaction-diffusion equations on stationary and evolving domains, surfaces and volumes; investigate the role of different reaction-kinetics in the bulk and on the surface and how these influence pattern formation during growth development; identify parameter values outside of the standard Turing spaces such that pattern generation occurs only in the presence of domain growth; investigate parameters or reaction-kinetics that give rise to non-standard reaction-kinetics that can only give rise to pattern formation during growth (or contraction) development and to investigate the effects of cross-diffusion for coupled systems of bulk-surface reaction-diffusion equations on stationary and evolving domains, surfaces and volumes.

Acknowledgements. This project (AM) has received funding from the European Union's Horizon 2020 research and innovation programme under the Marie Sklodowska-Curie grant agreement No 642866. This work (AM) is supported by the following grants: the Engineering and Physical Sciences Research Council (EP/J016780/1) on *Modelling, analysis and simulation of spatial patterning on evolving biological surfaces* and the Leverhulme Trust research project grant (RPG-2014-149) on *Unravelling new mathematics for 3D cell migration.* AM thanks the Isaac Newton Institute for Mathematical Sciences for its hospitality during the programme (Coupling Geometric PDEs with Physics for Cell Morphology, Motility and Pattern Formation; EPSRC EP/K032208/1). AM was partially supported by a fellowship from the Simons Foundation. AM is a Royal Society Wolfson Research Merit Award Holder, generously funded by the Wolfson Foundation and the Royal Society.

References

[1] Bangerth, W., Heister, T., Heltai, L., Kanschat, G., Kronbichler, M., Maier, M., Turcksin, B. and Young T.D. (2013). The `deal.II` Library, Version 8.1 *arXiv preprint.*

[2] Barreira R., Elliott C.M. and Madzvamuse A. (2011). The surface finite element method for pattern formation on evolving biological surfaces, *Journal of Math. Bio.* **63**, 1095-1119.

[3] Bianco, S., Tewes, F., Tajber, L., Caron, V., Corrigan, O.I. and Healy, A.M. (2013). Bulk, Surface properties and water uptake mechanisms of salt/acid amorphous composite systems. *Int. J. Pharm.* **456**:143-152.

[4] Chang, HR. and Grossman, R.L. (1999). Evaluation of bulk surface flux algorithms for light wind conditions using data from the Coupled Ocean-Atmosphere Response Experiment (COARE). *Q. J. R. Meteorol. Soc.* **125**:1551-1588.

[5] Chechkin, A.V., Zaid, I.M., Lomholt, M.A., Sokolov, I.M. and Metzler, R. (2012). Bulk-mediated diffusion on a planar surface: Full solution. *Phys. Rev. E.* **86**:041101.

[6] Dziuk, G. and Elliott, C.M. (2007). Surface finite elements for parabolic equations. *J. Comp. Math.* **25**:385-407.

[7] Elliott, C.M. and Ranner, T. (2012). Finite element analysis for a coupled bulk-surface partial differential equation. *IMA J. Num. Anal.* **33**(2):377-402.

[8] Elliott, C.M., Stinner, B. and Venkataraman, C. (2013). Modelling cell motility and chemotaxis with evolving surface finite elements. *J. Roy. Soc. Inter.* **9**(76):3027-3044.

[9] Garate, I. and Glazman, L. (2012). Weak localization and antilocalization in topological insulator thin films with coherent bulk-surface coupling. *Phys. Rev. B* **86**, 035422.

[10] Gierer, A. and Meinhardt, H. (1972). A theory of biological pattern formation. *Kybernetik.* **12**:30-39.

[11] Hahn, A. Held, K. and Tobiska, L. (2014). Modelling of surfactant concentration in a coupled bulk surface problem. *PAMM Proc. Appl. Math. Mech.* **14**:525-526.

[12] Hetzer, G., Madzvamuse, A. and Shen, W. (2012). Characterization of Turing diffusion-driven instability on evolving domains. *Discrete and Continuous Dynamical Systems* - Series A, **32**(11):3975-4000.

[13] Holmes, G.C. (2002). The use of hyperbolic cosines in solving cubic polynomials. *Mathematical Gazette*, **86**:473-477.

[14] Köster, D. Kriessl, O. and Siebert, K.G. (2008). Design of finite element tools for coupled surface and volume meshes. Mathematik. Technical Report, **2008-01**,

[15] Kwon, Y. and Derby J.J. (2001). Modeling the coupled effects of interfacial and bulk phenomena during solution crystal growth. *J. Cry. Growth.* **230**:328-335.

[16] Lakkis, O., Madzvamuse, A. and Venkataraman, C. (2013). Implicit–Explicit Timestepping with Finite Element Approximation of Reaction–Diffusion Systems on Evolving Domains *SINUM* **51**:2309-2330.

[17] Levine, H. and Rappel, W.J. (2005) Membrane-bound Turing patterns Phys. Rev. E **72**(6).

[18] Macdonald, C.B., Merrimanb, B. and Ruuth, S.J. (2013). Simple computation of reaction-diffusion processes on point clouds. *Proc. Nat. Acad. Sci.* **110**:9209-9214.

[19] Macdonald, G. Mackenzie, J.A. Nolan, M. and Insall, R.H. (2016). A computational method for the coupled solution of reaction?diffusion equations on evolving domains and manifolds: Application to a model of cell migration and chemotaxis. *Journal of Computational Physics.* **309**:207-226.

[20] Madzvamuse, A. (2000). A numerical approach to the study of spatial pattern formation. DPhil Thesis. University of Oxford.

[21] Madzvamuse, A., Gaffney, E.A. and Maini, P.K. (2010). Stability analysis of non-autonomous reaction-diffusion systems: The effects of growing domains. *Journal of Mathematical Biology*, **61**(1):133-164.

[22] Madzvamuse, A. and Chung, A.H.W. (2014). Fully implicit time-stepping schemes and non-linear solvers for systems of reaction-diffusion equations. *Appl. Math. Comp.*. **244**:361-374.

[23] Madzvamuse, A and Barreira, R (2014) Exhibiting cross-diffusion-induced patterns for reaction-diffusion systems on evolving domains and surfaces. *Physical Review E*, **90**. 043307-1-043307-14

[24] Madzvamuse A, Chung A.H.W. and Venkataraman C. (2015). Stability analysis and simulations of coupled bulk-surface reaction-diffusion systems. *Proc. Roy.* Soc. A. **471** (2175):20140546.

[25] Madzvamuse, A., Ndakwo, H.S. and Barreira, R. (2015). Cross-diffusion-driven instability for reaction-diffusion systems: analysis and simulations. *Journal of Mathematical Biology*, **70**(4):709-743.

[26] Madzvamuse, A. and Chung, A.H W (2016) The bulk-surface finite element method for reaction-diffusion systems on stationary volumes. *Finite Elements in Analysis and Design*, **108**:9-21.

[27] Madzvamuse, A. Ndakwo, H.S. and Barreira, R. (2016) Stability analysis of reaction-diffusion models on evolving domains: the effects of cross-diffusion. *Discrete and Continuous Dynamical Systems* - Series A, **36**(4):2133-217.

[28] Medvedev, E.S. and Stuchebrukhov, A.A. (2011). Proton diffusion along biological membranes. *J. Phys. Condens. Matter.* **23**:234103.

[29] Medvedev, E.S. and Stuchebrukhov, A.A. (2013). Mechanism of long-range proton translocation along biological membranes. *FEBS Lettes.* **587**:345-349.

[30] Murray J.D. (2003). Mathematical Biology II: Spatial models and biomedical applications. Third Edition. Springer.

[31] Nagata, W., Zangeneh, H.R.Z. and Holloway, D.M. (2013). Reaction-diffusion patterns in plant tip morphogenesis: bifurcations on spherical caps. . *Bull. Math. Biol.* **75**:2346-2371.

[32] Nisbet, D.R., Rodda, A.E., Finkelstein, D.I., Horne, M.K., Forsythe, J.S. and Shen, W. (2009). Surface and bulk characterisation of electrospun membranes: Problems and improvements. *Colloids and Surfaces B: Biointerfaces.* **71**:1-12.

[33] Novak, I.L., Gao, F., Choi, Y-S., Resasco, D., Schaff, J.C. and Slepchenko, B.M. (2007). Diffusion on a curved surface coupled to diffusion in the volume: Application to cell biology. J. Comp. Phys. **226**:1271-1290.

[34] Prigogine, I. and Lefever, R. (1968). Symmetry breaking instabilities in dissipative systems. II. *J. Chem. Phys.* **48**:1695-1700.

[35] Rätz, A. and Röger, M. (2012). Turing instabilities in a mathematical model for signaling networks. *J. Math. Biol.* **65**:1215-1244.

[36] Rätz, A. and Röger, M. (2013). Symmetry breaking in a bulk-surface reaction-diffusion model for signaling networks. *arXiv*:1305.6172v1.

[37] Rozada, I. Ruuth, S. and Ward, M.J. (2014). The stability of localized spot patterns for the Brusselator on the sphere. *SIADS*, **13**(1):564–627.

[38] Saad, Y. (2003). Iterative Methods for Sparse Linear Systems (2nd ed.). SIAM. pp. 231-234. ISBN 978-0-89871-534-7.

[39] Schnakenberg, J. (1979). Simple chemical reaction systems with limit cycle behaviour. *J. Theor. Biol.*, **81**:389-400.

[40] Tuncer, N. and Madzvamuse, A. (2016). Projected finite elements for systems of reaction-diffusion equations on closed evolving spheroidal surfaces. *Communications in Computational Physics.* Accepted.

[41] Turing, A. (1952). On the chemical basis of morphogenesis. *Phil. Trans. Royal Soc. B.* **237**: 37-72.

[42] Van der Vorst, H. A. (1992). A Fast and Smoothly Converging Variant of Bi-CG for the Solution of Nonsymmetric Linear Systems. *SIAM J. Sci. and Stat. Comput.* **13** (2): 631-644. doi:10.1137/0913035.

[43] Venkataraman, C., Lakkis, O. and Madzvamuse, A. (2012). Global existence for semilinear reaction-diffusion systems on evolving domains *J. Math. Biol.***64**:41-67.

[44] Venkataraman, C. Sekimura, T. Gaffney, E.A. Maini, P.K. and Madzvamuse, A. (2011). Modeling parr-mark pattern formation during the early development of Amago trout. *Phys. Rev. E*, **8**4(4): 041923.

(a) $t = 0$

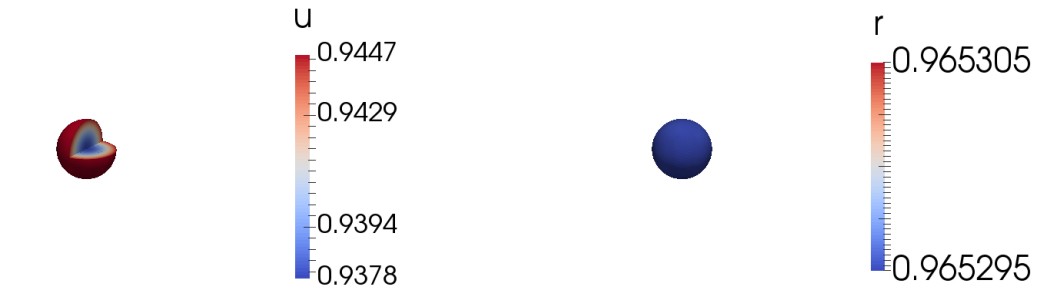

(b) $t = 6$

(c) $t = 15$

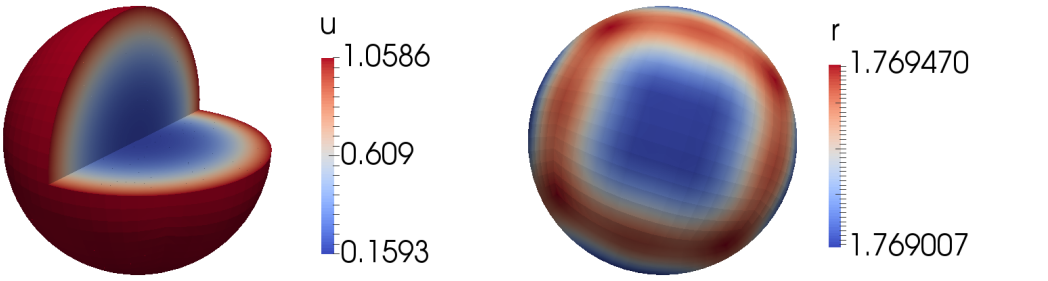

(d) $t = 25$

FIGURE 5. Numerical solutions corresponding to the coupled system of BSRDEs (2.1)-(2.14) with *activator-depleted* kinetics for $d_\Omega = 20$ in the bulk and $d_\Gamma = 20$ on the surface and scaling parameters $\gamma_\Omega = \gamma_\Gamma = 1$. Column 1: solutions in the bulk representing u and Columns 2: solutions on the surface representing r. We observe stripe pattern formation in the bulk and circular patterns on the surface. (Colour figure online).